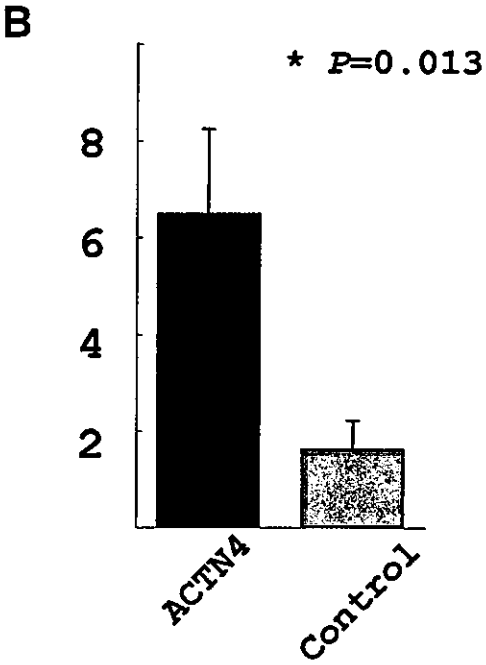

Figure 8. (*A*) Findings on laparotomy in a SCID mouse that had received an injection of DLD1 Tet-off ACTN4 cells into its spleen 5 weeks earlier. *Arrows* indicate metastatic nodules. (*B*) Mean numbers of metastatic nodules per mouse formed by the injection of DLD1 Tet-off ACTN4 (n = 8) and DLD1 Tet-off control (n = 8) (P = .013; Student t test). *Error bars* represent the SEM.

P = .001) than among all 41 cases (5/13 in stage II vs 23/28 in stages III–IV [IV = any T, any N, M1]; P = .010).

Discussion

Cell movement can be viewed as a dynamic multistep cycle of (1) extension of podia, (2) attachment of the leading edge of podia to the substrate, (3) forward retraction of the cell body, and (4) detachment of rear adhesions.[30] Although the molecular mechanisms of podia formation are not perfectly understood, a certain set of actin-binding proteins seems to be involved, because filamentous actin is highly concentrated in the leading edge of podia.[10–13] In this study, we showed that DLD1 Tet-off ACTN4 cells dramatically extended filopodia (Figure 3) after the removal of Dox from the culture medium. Scanning electron microscopy revealed the formation of membrane ruffles at the leading edge of the filopodia (Figure 4), and confocal immunofluorescence microscopy revealed that actinin-4 protein was concentrated in these membrane ruffles (Figure 5). We included a mock transfectant in every experiment to avoid any unexpected effects of Dox. The removal of Dox had no significant morphologic effects on the DLD1 Tet-off control cells. All of the above data confirmed that acti-

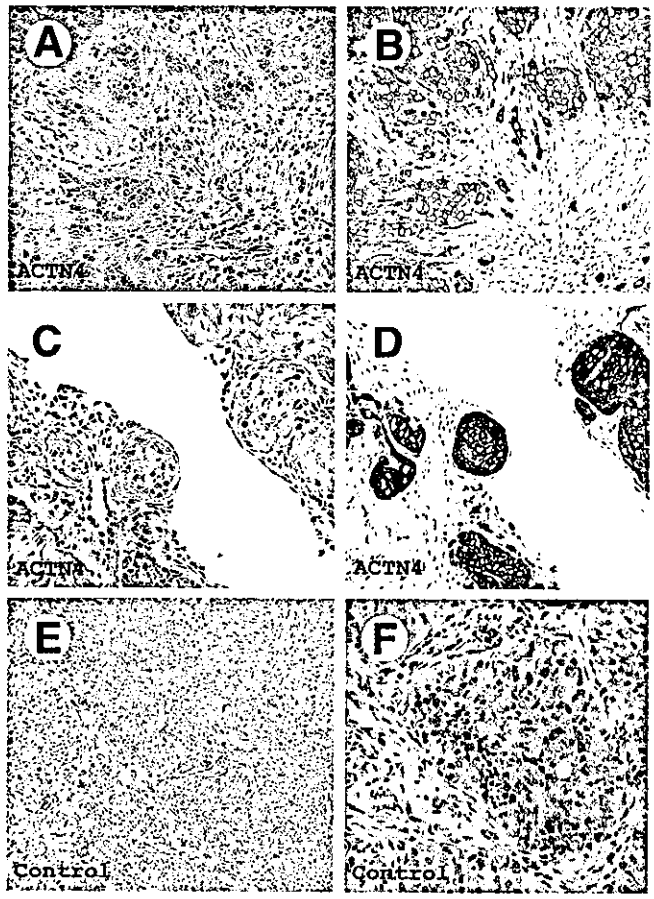

Figure 9. Histology of tumors formed in SCID mice by the injection of (*A–D*) DLD1 Tet-off ACTN4 and (*E* and *F*) DLD1 Tet-off control cells. (*A* and *B*) A tumor that formed in the splenic hilum after the injection of DLD1 Tet-off ACTN4. (*C* and *D*) Tumor emboli of DLD1 Tet-off ACTN4 in lymphatic vessels of the peritoneum. (*E* and *F*) Tumors that formed in the splenic hilum after the injection of DLD1 Tet-off control. (*A*, *C*, *E*, and *F*) H&E staining and (*B* and *D*) immunostaining with anti-HA antibody. (Original magnification: *A–E*, 100×; *F*, 200×.)

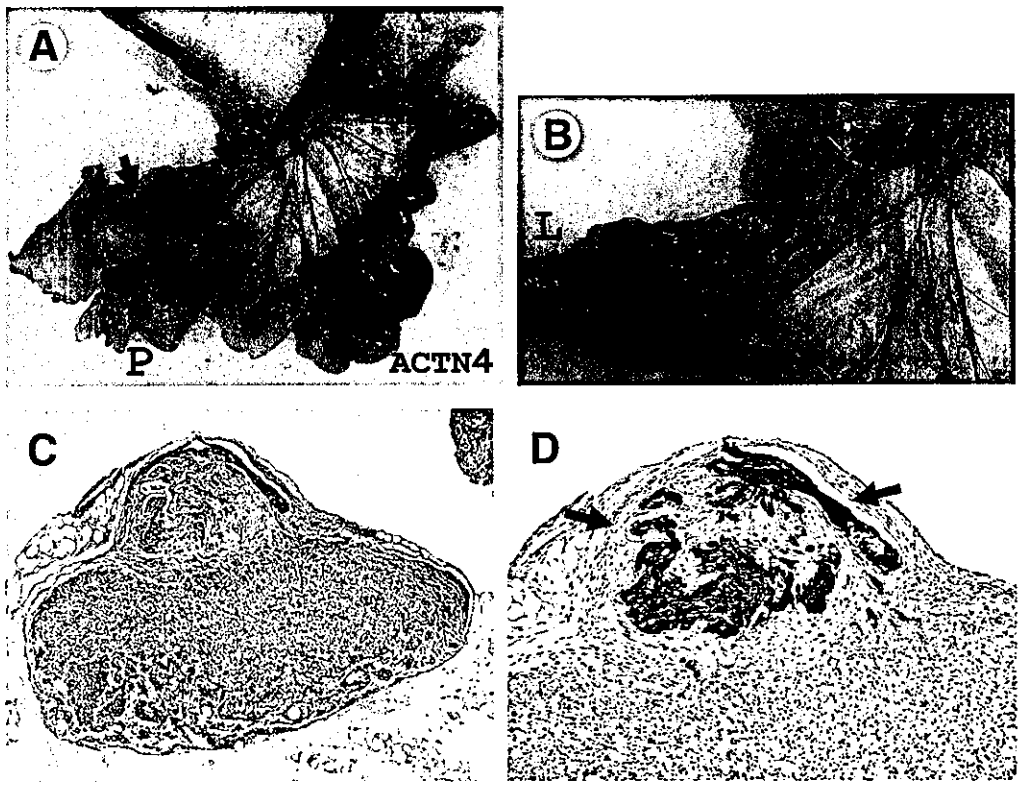

Figure 10. (*A* and *B*) Colon and mesentery of a SCID mouse that had received an orthotopic implantation of DLD1 Tet-off ACTN4 cells into its mesocecum 5 weeks earlier. P, primary tumor; L, lymph node metastases. (*C* and *D*) Histology of a regional mesenteric lymph node with metastasis. (*C*) H&E staining, and (*D*) immunostaining with anti-HA antibody. *Arrows* indicate tumor emboli in lymphatic vessels. (Original magnification: *C*, 40×; *D*, 100×.)

nin-4 was actively involved in the "extension of podia" step in cell movement.

Classic nonmuscle actinin, actinin-1, seems to be essential for the stabilization of cell adhesion by connecting the actin cytoskeleton to focal adhesions and adherens junctions via integrin-β1 and α-catenin, respectively.[17,18,31] Despite a high similarity in their amino acid sequences, the 2 nonmuscle actinins are not functionally redundant. Kaplan et al identified mutations in the actinin-4 gene (*ACTN4*) causative for familial focal segmental glomerulosclerosis.[32] Mice deficient in the actinin-4 gene were shown to manifest severe glomerular disease resembling focal segmental glomerulosclerosis.[33] The failure of foot process extension by glomerular podocytes is believed be the major cause of focal segmental glomerulosclerosis. Actinin-4 was localized in the sharply extended cell processes of cultured podocytes, where filamentous actin bundles were concentrated.[34] Filopodia extension in motile cells may use a molecular machinery similar to that of foot process extension in glomerular podocytes.

We observed that the level of actinin-4 protein expression was increased in colorectal cancer cells compared with levels in normal cells from the same patients (Figure 1). The increased expression of actinin-4 was most significant in the focally dedifferentiated cancer cells at the invasive front (Figure 2), where E-cadherin–mediated cell adhesion was diminished and the cancer cells had acquired motility.[35,36] Focal dedifferentiation was frequently observed in cases with an unfavorable prognosis.[28] We were able to reproduce the histology resembling focal dedifferentiation in animal models in vivo using DLD1 Tet-off ACTN4 (Figure 9*A* and *B*).

The wound-healing assay revealed that DLD1 Tet-off ACTN4 dramatically increased cell motility after the removal of Dox (Figure 6). However, although statistically significant, the increment in cell motility was rather modest when assessed using the ArrayScan assay (Figure 7). In parental DLD1 cells, E-cadherin–mediated cell adhesion was well maintained and cell motility was relatively low (data not shown). Cells were trypsinized in the presence of EDTA to obtain a single cell suspension before use in the assay; this procedure probably disrupted E-cadherin–mediated cell adhesion, resulting in an underestimation. Kos et al reported that the motility of lymphocytes derived from *Actn4*$^{-/-}$ mice was increased in a chemotaxis assay compared with the motility of lymphocytes from *Actn4*$^{+/+}$ mice.[33] A direct comparison of this result with ours is difficult because they used nonepithelial cells, and chemotaxic activity is largely determined by integrin-mediated cell adhesion.

When injected orthotopically into the mesocecum of SCID mice, DLD1 Tet-off ACTN4 cells metastasized into the regional mesenteric lymph nodes (Figure 10),

resembling the behavior of clinical colorectal cancer. Liver metastasis was not observed in any of the animals as revealed by histologic examination. The parental DLD1 cells were shown to have a tumorigenic ability when injected directly into the liver of SCID mice[26] but rarely metastasized to the liver, even after splenic injection.[37] Splenic injection is known to mechanically convey tumor cells into the portal vein. From these observations, we speculated that the increased expression of actinin-4 might not be sufficient for the extravasation of circulating tumor cells out of vascular vessels. The lymphatic endothelium, on the other hand, may be more susceptible to the penetration of DLD1 cells than the vascular endothelium.

Consistent with the animal experiments, we found that the increased expression of actinin-4 in focally dedifferentiated cancer cells from 41 patients with colorectal cancer was significantly correlated with lymph node metastasis but not with organ metastasis (Table 1). Among the patients without organ metastasis (stages II and III), lymph node metastasis was observed only in cases with an increased expression of actinin-4 in focally dedifferentiated cancer cells (Table 1). These findings suggest that organ metastasis is mediated by some undetermined molecular mechanisms other than actinin-4. We previously reported that the subcellular localization of actinin-4 was significantly correlated with a poorer prognosis in patients with breast cancer.[16] Another report also found that the increased expression of actinin-4 was the most significant predictor of non–small cell lung cancer prognosis using a large-scale microarray analysis.[20] The expression of actinin-4 was increased in colorectal cancer cells, especially in the invasive front. Recently, we observed a similar tendency in pancreatic cancer (manuscript in preparation). Based on these findings, we believe that actinin-4 may be universally involved in the metastasis of various cancers.

In conclusion, we showed that actinin-4 significantly changes cell motility and cell appearance. We frequently observed emboli of DLD1 Tet-off ACTN4 cells in the lymphatic vessels of SCID mice, as shown in Figure 9*C* and *D* and Figure 10*C* and *D*. The enhanced motility likely increases the chances of tumor cells migrating into lymphatic vessels. We also raise the possibility that an increase in cell shape plasticity may be necessary for the tumor cells to penetrate the tiny gaps between lymphatic endothelial cells. We conclude that the suppression of actinin-4 expression or functional intervention may inhibit the lymphatic spread of colorectal cancer and should be considered as a new molecular target for the prevention of lymph node metastasis of colorectal cancer.

References

1. Kadry Z, Clavien PA. New treatments with curative intent for metastatic colorectal liver cancer. Expert Opin Pharmacother 2002;8:1191–1197.
2. Curley SA, Izzo F, Abdalla E, Vauthey JN. Surgical treatment of colorectal cancer metastasis. Cancer Metastasis Rev 2004;1–2: 165–182.
3. Van Roy F, Mareel M. Tumour invasion: effects of cell adhesion and motility. Trends Cell Biol 1992;2:163–169.
4. Banyard J, Zetter BR. The role of cell motility in prostate cancer. Cancer Metastasis Rev 1998;-9917:449–458.
5. Genda T, Sakamoto M, Ichida T, Asakura H, Kojiro M, Narumiya S, Hirohashi S. Cell motility mediated by rho and Rho-associated protein kinase plays a critical role in intrahepatic metastasis of human hepatocellular carcinoma. Hepatology 1999;30:1027–1036.
6. Partin AW, Schoeniger JS, Mohler JL, Coffey DS. Fourier analysis of cell motility: correlation of motility with metastatic potential. Proc Natl Acad Sci U S A 1989;86:1254–1258.
7. Lauffenburger DA, Horwitz AF. Cell migration: a physically integrated molecular process. Cell 1996;84:359–369.
8. Wells A. Tumor invasion: role of growth factor-induced cell motility. Adv Cancer Res 2000;78:31–101.
9. Gumbiner BM. Cell adhesion: the molecular basis of tissue architecture and morphogenesis. Cell 1996;84:345–357.
10. Pantaloni D, Le Clainche C, Carlier MF. Mechanism of actin-based motility. Science 2001;292:1502–1506.
11. Nobes CD, Hall A. Rho, rac, and cdc42 GTPases regulate the assembly of multimolecular focal complexes associated with actin stress fibers, lamellipodia, and filopodia. Cell 1995;81:53–62.
12. Pollard TD, Blanchoin L, Mullins RD. Molecular mechanisms controlling actin filament dynamics in nonmuscle cells. Annu Rev Biophys Biomol Struct 2000;29:545–576.
13. Miki H, Takenawa T. Regulation of actin dynamics by WASP family proteins. J Biochem (Tokyo) 2003;134:309–313.
14. Millake DB, Blanchard AD, Patel B, Critchley DR. The cDNA sequence of a human placental alpha-actinin. Nucleic Acids Res 1989;17:6725.
15. Beggs AH, Byers TJ, Knoll JH, Boyce FM, Bruns GA, Kunkel LM. Cloning and characterization of two human skeletal muscle alpha-actinin genes located on chromosomes 1 and 11. J Biol Chem 1992;267:9281–9288.
16. Honda K, Yamada T, Endo R, Ino Y, Gotoh M, Tsuda H, Yamada Y, Chiba H, Hirohashi S. Actinin-4, a novel actin-bundling protein associated with cell motility and cancer invasion. J Cell Biol 1998;140:1383–1393.
17. Miyamoto S, Teramoto H, Coso OA, Gutkind JS, Burbelo PD, Akiyama SK, Yamada KM. Integrin function: molecular hierarchies of cytoskeletal and signaling molecules. J Cell Biol 1995; 131:791–805.
18. Knudsen KA, Soler AP, Johnson KR, Wheelock MJ. Interaction of alpha-actinin with the cadherin/catenin cell-cell adhesion complex via alpha-catenin. J Cell Biol 1995;130:67–77.
19. Araki N, Hatae T, Yamada T, Hirohashi S. Actinin-4 is preferentially involved in circular ruffling and macropinocytosis in mouse macrophages: analysis by fluorescence ratio imaging. J Cell Sci 2000;113:3329–3340.
20. Yamagata N, Shyr Y, Yanagisawa K, Edgerton M, Dang TP, Gonzalez A, Nadaf S, Larsen P, Roberts JR, Nesbitt JC, Jensen R, Levy S, Moore JH, Minna JD, Carbone DP. A training-testing approach to the molecular classification of resected non-small cell lung cancer. Clin Cancer Res 2003;9:4695–4704.

21. Teramoto H, Malek RL, Behbahani B, Castellone MD, Lee NH, Gutkind JS. Identification of H-Ras, RhoA, Rac1 and Cdc42 responsive genes. Oncogene 2003;22:2689–2697.
22. Yamada T, Takaoka AS, Naishiro Y, Hayashi R, Maruyama K, Maesawa C, Ochiai A, Hirohashi S. Transactivation of the multidrug resistance 1 gene by T-cell factor 4/beta-catenin complex in early colorectal carcinogenesis. Cancer Res 2000;60:4761–4766.
23. Shimoyama Y, Hirohashi S, Hirano S, Noguchi M, Shimosato Y, Takeichi M, Abe O. Cadherin cell-adhesion molecules in human epithelial tissues and carcinomas. Cancer Res 1989;49:2128–2133.
24. Naishiro Y, Yamada T, Takaoka AS, Hayashi R, Hasegawa F, Imai K, Hirohashi S. Restoration of epithelial cell polarity in a colorectal cancer cell line by suppression of beta-catenin/T-cell factor 4-mediated gene transactivation. Cancer Res 2001;61:2751–2758.
25. Dexter DL, Spremulli EN, Fligiel Z, Barbosa JA, Vogel R, VanVoorhees A, Calabresi P. Heterogeneity of cancer cells form a single human colon carcinoma. Am J Med 1981;71:949–956.
26. Yasui N, Sakamoto M, Ochiai A, Ino Y, Akimoto S, Orikasa A, Kitajima M, Hirohashi S. Tumor growth and metastasis of human colorectal cancer cell lines in SCID mice resemble clinical metastatic behaviors. Invasion Metastasis 1997;17:259–269.
27. Ino Y, Gotoh M, Sakamoto M, Tsukagoshi K, Hirohashi S. Dysadherin, a cancer-associated cell membrane glycoprotein, down-regulates E-cadherin and promotes metastasis. Proc Natl Acad Sci U S A 2002;99:365–370.
28. Ono M, Sakamoto M, Ino Y, Moriya Y, Sugihara K, Muto T, Hirohashi S. Cancer cell morphology at the invasive front and expression of cell adhesion-related carbohydrate in the primary lesion of patients with colorectal carcinoma with liver metastasis. Cancer 1996;78:1179–1186.
29. Sobin LH, Wittekind CH. TNM classification of malignant tumours. 5th ed. New York: Wiley, 1997.
30. Webb DJ, Parsons JT, Horwitz AF. Adhesion assembly, disassembly and turnover in migrating cells—over and over and over again. Nat Cell Biol 2002;4:E97–E100.
31. Burridge K, Nuckolls G, Otey C, Pavalko F, Simon K, Turner C. Actin-membrane interaction in focal adhesions. Cell Differ Dev 1990;32:337–342.
32. Kaplan JM, Kim SH, North KN, Rennke H, Correia LA, Tong HQ, Mathis BJ, Rodriguez-Perez JC, Allen PG, Beggs AH, Pollak MR. Mutations in ACTN4, encoding alpha-actinin-4, cause familial focal segmental glomerulosclerosis. Nat Genet 2000;24:251–256.
33. Kos CH, Le TC, Sinha S, Henderson JM, Kim SH, Sugimoto H, Kalluri R, Gerszten RE, Pollak MR. Mice deficient in alpha-actinin-4 have severe glomerular disease. J Clin Invest 2003;111:1683–1690.
34. Welsch T, Endlich N, Kriz W, Endlich K. CD2AP and p130Cas localize to different F-actin structures in podocytes. Am J Physiol Renal Physiol 2001;281:F769–F777.
35. Hirohashi S, Kanai Y. Cell adhesion system and human cancer morphogenesis. Cancer Sci 2003;94:575–581.
36. Inomata M, Ochiai A, Sugihara K, Moriya Y, Yamaguchi N, Adachi Y, Kitano S, Hirohashi S. Macroscopic features at the deepest site of tumor penetration predicting liver metastases of colorectal cancer. Jpn J Clin Oncol 1998;28:123–128.
37. Tibbetts LM, Doremus CM, Tzanakakis GN, Vezeridis MP. Liver metastases with 10 human colon carcinoma cell lines in nude mice and association with carcinoembryonic antigen production. Cancer 1993;71:315–321.

Received May 17, 2004. Accepted September 23, 2004.

Address requests for reprints to: Tesshi Yamada, M.D., Ph.D., Chemotherapy Division, National Cancer Center Research Institute, 5-1-1 Tsukiji Chuoh-ku, Tokyo 104-0045, Japan. e-mail: tyamada@ncc.go.jp; fax: (81) 3-3547-6045.

Supported by grants from the Ministry of Health, Labor and Welfare and by the Program for the Promotion of Fundamental Studies in Health Sciences of the Organization for Pharmaceutical Safety and Research of Japan. Y. H. is a recipient of the Research Resident Fellowship from the Foundation for the Promotion of Cancer Research.

Oncogene (2004) 23, 5257–5262

www.nature.com/onc

Alternative splice variant of actinin-4 in small cell lung cancer

Kazufumi Honda[1], Tesshi Yamada*[,1], Masahiro Seike[1], Yasuharu Hayashida[1], Masashi Idogawa[1], Tadashi Kondo[1], Yoshinori Ino[1] and Setsuo Hirohashi[1]

[1]*Cancer Proteomics Project, National Cancer Center Research Institute, 5-1-1 Tsukiji, Chuo-ku, Tokyo 104-0045, Japan*

Tumor-associated alternative RNA splicing has gained considerable attention. We identified a novel alternative splice variant RNA of actinin-4 in human small cell lung caner (SCLC). Expression of the splice variant was highly specific to SCLC cell lines (10/10), biopsies (3/3), and testis. The variant encoded a peptide with a three amino-acid change in exon 8, where the germline missense mutation takes place in familial focal segmental glomerulosclerosis (FSGS). The variant protein showed high affinity to filamentous actin polymers and was not localized with cortical actin. Alternatively spliced actinin-4 may be a new diagnostic marker of SCLC and a candidate target for selective therapy.
Oncogene (2004) **23**, 5257–5262. doi:10.1038/sj.onc.1207652
Published online 3 May 2004

Keywords: actin; actinin-4; alternative splicing; cancer-testis antigen; small-cell lung cancer

Lung cancer is the leading cause of cancer death in Japan and Western countries (Levi *et al.*, 1996). Lung caner can be divided into four major histological subtypes, including squamous cell carcinoma, adenocarcinoma, large cell carcinoma, and small cell carcinoma (SCLC) (Carney *et al.*, 1985). SCLC is distinguished from the other three histological subtypes (non-SCLC) by its distinct histological appearance and early metastasis to lymph nodes, the central nervous system, bone and other sites (Carney *et al.*, 1985; Shimosato *et al.*, 1986). Although cancer metastasis is a multifactorial biological phenomenon, disrupted cell adhesion and enhanced cell motility are considered to be pivotal (Behrens *et al.*, 1992). Histopathologically, SCLC is characterized by scant cytoplasm and a high nuclear/cytoplasmic ratio (Arora *et al.*, 2003). SCLC cells are known to be fragile and highly susceptible to the mechanical force applied during biopsy procedures (Arora *et al.*, 2003). SCLC cells in culture adhere poorly to the plastic surface and often grow in suspension (Carney *et al.*, 1985). Based on these observations, we hypothesized that SCLC may contain abnormalities in the actin cytoskeleton, because the status of actin directly affects cellular morphology, solidity, adhesion, and motility (Small *et al.*, 1999; Hirohashi and Kanai, 2003).

The actin cytoskeleton is regulated by various kinds of actin-binding proteins. We previously isolated α-actinin-4 as a novel actin-binding protein (Honda *et al.*, 1998). Increased expression and altered subcellular localization of actinin-4 were associated with cell motility and cancer metastasis (Honda *et al.*, 1998; Araki *et al.*, 2000). Reduced expression of actinin-4 is reportedly associated with cell adhesion abnormalities in neuroblastoma cell lines (Nikolopoulos *et al.*, 2000).

Status of the actin cytoskeleton and actinin-4 protein in SCLC

To evaluate the above hypothesis, we first examined the status of the actin cytoskeleton and actinin-4 protein in SCLC (five cases) and non-SCLC (10 cases) by fluorescence immunohistochemistry (Figure 1a–i). In acetone-fixed and paraffin-embedded tissues, filamentous actin polymers appeared to be well preserved and were stained *in vivo* with fluorescence-labeled phalloidin. The cortical actin cytoskeleton uniformly underlined cell membranes in all 10 non-SCLC cases (red, squamous cell carcinoma, Figure 1a and adenocarcinoma, Figure 1d). However, the actin cytoskeleton of SCLC was irregularly interrupted or fragmented and the staining intensity was not uniform (red, Figure 1g).

The actinin-4 protein was dissociated from the cortical actin cytoskeleton and translocated into the nucleus in all SCLC cases (Figure 1h and i). Immunoblotting revealed no significant gross alterations in actinin-4 or β-actin proteins extracted from SCLC and non-SCLC cell lines (Figure 1j).

Identification of the alternative splice variant of actinin-4

We next sequenced nearly the entire coding region of actinin-4 cDNA obtained from two SCLC cell lines, H69 and H231. We noticed a mixture of two different sequences appearing in nucleotides 793–872 (NM_004924.2) (top, Figure 2a). The two transcripts were separately cloned and their nucleotide sequences were determined (Ub and Va, Figure 2a). One transcript

*Correspondence: T Yamada; E-mail: tyamada@gan2.res.ncc.go.jp
Received 18 September 2003; revised 17 February 2004; accepted 19 February 2004; published online 3 May 2004

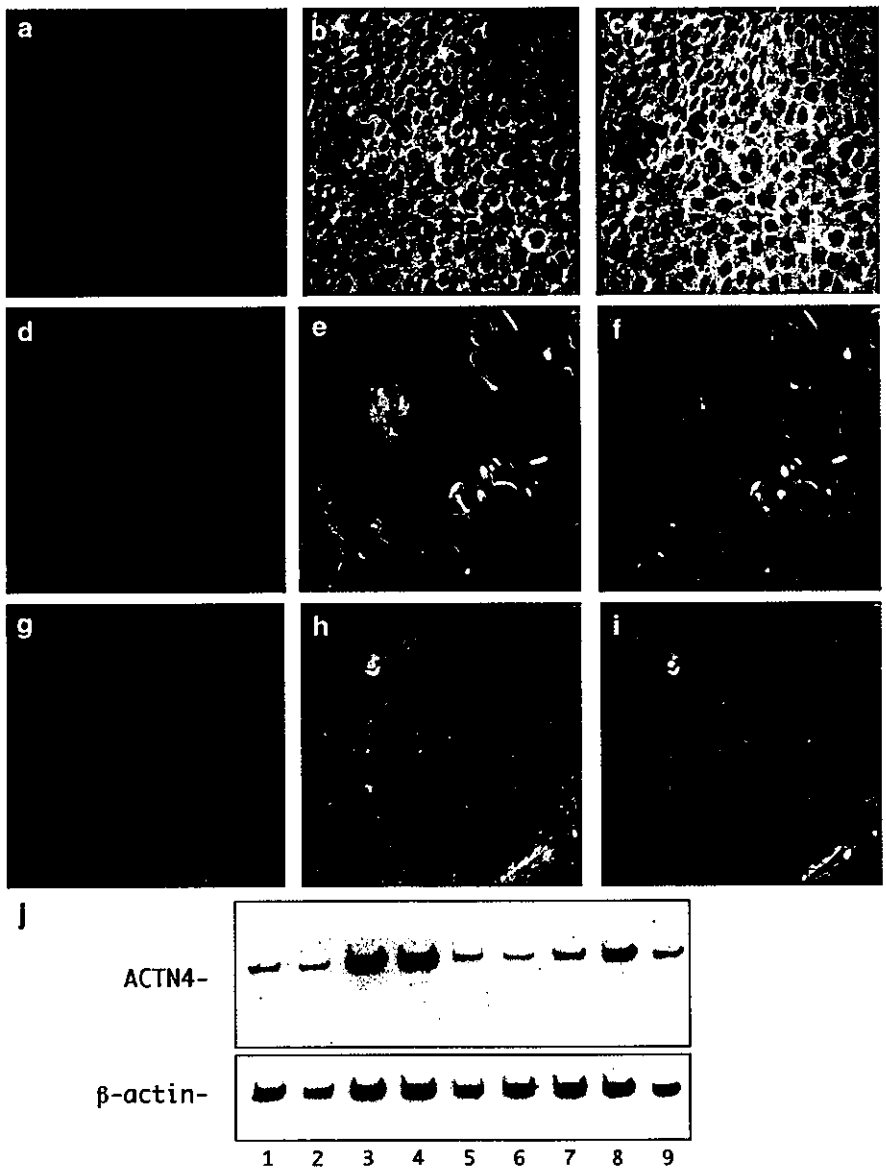

Figure 1 Fluorescence immunohistochemistry and immunoblot analyses of SCLC (**a–i**) Fluoresence immunohistochemistry showing the subcellular localization of actin filaments (red, **a**, **d**, and **g**) and the actinin-4 protein (green, **b**, **e**, and **h**) in squamous cell carcinoma (**a–c**), adenocarcinoma (**d–f**), and SCLC (**g–i**). After deparaffinization, acetone-fixed and paraffin-embedded tissue sections were incubated overnight with anti-actinin-4 monoclonal antibody, NCC-Lu632 (Honda *et al.*, 1998). Actin filaments (**a**, **d**, and **g**) and the actinin-4 protein (**b**, **e**, and **h**) were visualized with Alexa Flour 594 phalloidin and Alexa Flour 488 anti-mouse IgG (Molecular Probes, Eugene, OR, USA), respectively. Merged images of actinin-4 (green) and actin filaments (red) are presented in (**c**), (**f**), and (**i**). Original magnification was × 100. (**j**) Immunoblot analysis of the actinin-4 protein extracted from non-SCLC (lanes 1–5) and SCLC (lanes 6–9). Lane 1, PC1; lane 2, PC3; lane 3, PC9; lane 4, PC10; lane 5, PC13; lane 6, Lu130; lane 7, Lu134; lane 8, Lu135 and lane 9, Lu139. Immunoblotting was performed using anti-actinin-4 polyclonal (ACTN4)(Honda *et al.*, 1998) and anti-β-actin monoclonal (β-actin) (Abcam, Cambridge, UK) antibodies

(Ub, hereafter, ubiquitous type, Figure 2a) was the same sequence as one we previously reported (Honda *et al.*, 1998) and the other (Va, variant type, Figure 2a) was distinct from the formerly described sequence of the actinin-4 transcript.

Comparison of the nucleotide sequence of the variant transcript with the genomic sequence of actinin-4 (*ACTN4*, NT_011109.15) revealed RNA alternative splicing to apparently be responsible for generation of the variant transcript. The 83-bp exon 8 of the actinin-4 gene was replaced by a new exon of the same size (8′) that exists in intron 8 (Figure 2b). This is a putative exon based on its being flanked by conserved splicing acceptor and donor sequences (data not shown). No mutation in the region of exon/intron boundaries of exons 8, 8′, and 9 was detected by sequencing genomic DNA of H69 and N231 cells (data not shown).

The nucleotide change in the variant transcript was predicted to produce a new restriction site for *Ban*II. The presence or absence of the variant transcript was determined in a larger panel of samples by digesting PCR products of actinin-4 cDNA with *Ban*II

(Figure 2c). The variant RNA splicing was detected consistently in all 10 SCLC cell lines examined (H69, N230, N231, N471, Lu130, Lu134A, Lu134B, Lu140, Lu141, and Lu143), but not in any of the 10 non-SCLC cell lines (PC1, PC3, PC7, PC9, PC10, PC13, Lu99, Lu65A, Lu65F, and Lu90) (top, Figure 2c), human fibroblast WI-26, foreskin keratinocyte, or a panel of 12 cell lines derived from myeloid leukemia, mesothelioma, gastric cancer, colorectal cancer, ovarian cancer, vulvar cancer, and pancreatic cancer (data not shown). In normal organs examined (middle, Figure 2c), the variant transcript was detectable in the testis (lane T) and there was a trace amount in the brain (lane B). The variant transcript was not detected in any other normal organs. The variant transcript was detected in all three tissue samples of surgically resected SCLC but not in any of seven samples of non-SCLC (bottom, Figure 2c) or normal lung (data not shown).

Although the new exon 8′ had sequence similarity to the usual exon 8 (62/83, 74.4%), the variant type was predicted to encode a polypeptide differing from ubiquitous type in three amino acids (Figure 2d): asparagine (amino acid 248, NP_004915) to glycine, alanine (250) to leucine, and serine (262) to cysteine. Kaplan *et al.* (2000) reported the missense mutations in exon 8 of the actinin-4 gene in three familial focal segmental glomerulosclerosis (FSGS) families and this mutation was confirmed to be causative for FSGS in an animal model (Michaud *et al.*, 2003). The three altered amino-acid sites seen in the splice variant of actinin-4 were adjacent to those of point mutations reported in FSGS (Figure 2d).

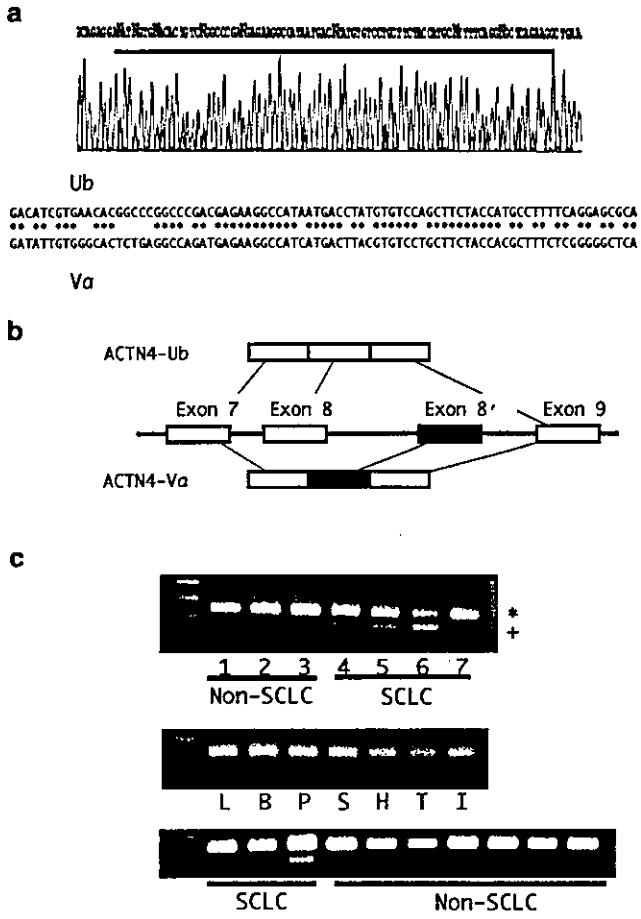

In-vitro actin-binding activity of variant actinin-4

The actinin-4 protein with the missense mutation in exon 8 in FSGS has been reported to have a high affinity to filamentous actin polymers. We compared the actin-binding activity of ubiquitous and variant types of recombinant actinin-4 proteins, including the minimal actin-binding and pleckstrin-homology (PH) domains and splicing sites (Figure 3a). After incubation with filamentous actin polymers, insoluble materials were precipitated with ultracentrifugation and examined by immunoblotting with anti-actinin-4 rabbit polyclonal antibody (top, Figure 3b). Like mutant actinin-4 in FSGS, the variant actinin-4 bound to filamentous actin

Figure 2 Two distinct transcripts of actinin-4 in SCLC (**a**) Sequence of actinin-4 cDNA of the SCLC cell line H69. A 1-μg sample of DNase-I treated total RNA were reverse-transcribed, amplified by PCR using a pair of primers, ACCAGTCGTACCAGTACGGC (ACTN4-F2) and AGATACAGAGTGGAGGAATGGG (ACTN4-R2), and directly sequenced using primers covering the entire coding region, including the ACTN4-F3 primer CCGTATAAGAACGT CAATGTGC. Blue line indicates the region where two sequences overlap. Fragments (339 bp) of actinin-4 cDNA (nucleotides 594-932, NM_004924.2) were amplified by PCR using a pair of primers, ACTN-F3 and GTTCTCTTGGTTGACAGCCAGC (ACTN4-R4), cloned and sequenced using T7 primer. Sequence of ubiquitous actinin-4 (Ub) is aligned with that of variant (Va) actinin-4 cDNA cloned from H69. (**b**) Schematic representation of alternative exon usage by the ubiquitous (top) and variant (bottom) transcripts in SCLC. (**c**) Detection of variant transcript in lung cancer cell lines (top), normal human tissues (middle) and surgically resected lung cancer tissues (bottom). Fragments (339 bp) of actinin-4 cDNA (nucleotides 594–932) were amplified by PCR using a pair of primers, ACTN-F3 and ACTN4-R4. Ubiquitous (*, 339 bp) and variant types (+, 280 bp) of cDNA fragments of actinin-4 are detected by digestion with a restriction enzyme, *BanII*. Lane 1, Lu65; lane 2, PC9; lane 3, Lu90; lane 4, H69; lane 5, N231; lane 6, Lu130 and lane 7, Lu143; lane L, liver; lane B, brain; lane P, placenta; lane S, spleen; lane H, heart; lane T, testis and lane I, small intestine. Human total RNA of normal tissues was obtained from OriGene, Rockville, MA, USA. (**d**) Alignment of deduced amino-acid sequences of ubiquitous and variant actinin-4 proteins in SCLC (top), mutated actinin-4 in three FSGS families (middle), and all four human actinin proteins (bottom). The amino-acid changes in variant actinin-4 occur in the region conserved among the four actinins

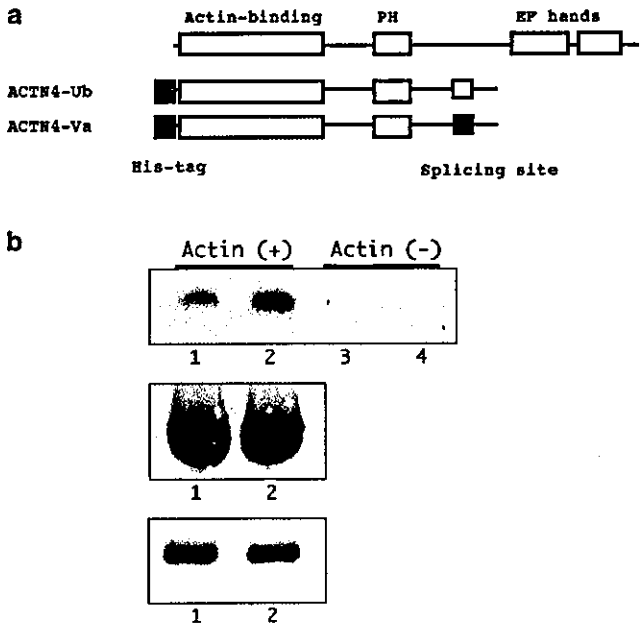

Figure 3 Different actin-binding activity of variant actinin-4. (**a**) Schematic representation of recombinant ubiquitous and variant actinin-4 proteins. His-tagged fusion proteins of actinin-4 (amino acids 28–235) were expressed using the Rapid Translation System RTS 500 Instrument (Roche Molecular Biochemicals, Mannheim, Germany) and affinity-purified on the His MicroSpin Purification Module (Amersham Biosciences, Amersham, UK). (**b**) The actin-binding activity of purified actinin-4 proteins was analysed using an Actin Binding Protein Biochem kit (Cytoskeleton, Acoma, CO, USA). Briefly, 2 μg of recombinant proteins of ubiquitous (lanes 1 and 3) and variant (lanes 2 and 4) actinin-4 were incubated with (lanes 1 and 2) or without (lanes 3 and 4) 23 μM filamentous actin polymers at room temperature for 30 min and sedimented at $1.5 \times 10^5 g$ for 1.5 h at 24°C. Precipitated actinin-4 proteins are detected by immunoblotting with anti-actinin-4 polyclonal antibody (top). Coomassie blue staining and immunoblotting reveal the equivalent precipitation of filamentous actin polymers (middle) and the equivalent input of actinin-4 proteins (bottom), respectively, in lanes 1 and 2

polymers more strongly than did ubiquitous actinin-4 (lanes 1 and 2, Figure 3b). In the absence of actin polymers, actinin-4 was not precipitated (lanes 3 and 4). Precipitated filamentous actin polymers and input recombinant actinin-4 proteins were almost equivalent as shown by coomassie blue staining (middle, Figure 3b) and immunoblotting with anti-actinin-4 antibody (bottom, Figure 3b), respectively.

Functional properties of variant actinin-4

Finally, to gain insight into the functional properties of variant actinin-4, we compared the subcellular localization of two types of actinin-4. We transiently transfected NIH 3T3 cells with variant and ubiquitous types of near full-length actinin-4 cDNA constructs tagged NH2-terminally with enhanced green fluorescence protein (EGFP) (Figure 4a–f). Ubiquitous type actinin-4 was co-localized with cortical filamentous actin bundles in membrane ruffling, especially at the periphery of leading edges (Figure 4a and green, 4c). In contrast, the splice variant of actinin-4 was not concentrated along the cell membrane and was found to be co-localized mainly with actin stress fibers (Figure 4d and green, 4f). As revealed by phalloidin staining, stress fiber formation appeared to be enhanced in cells transfected with the variant construct of actinin-4 (Figure 4e and red, 4f), probably because of its higher filamentous actin polymer cross-linking activity. The dissociation from cortical actin is consistent with the results of the above immunohistochemical analyses (Figure 1a–i), but we observed no nuclear translocation of exogenously expressed variant actinin-4 in NIH3T3 cells.

Concluding remarks

Alternative RNA splicing may affect the native functions of proteins. α-Actinin is a family of proteins that bind and crosslink filamentous actin polymers (Djinovic-Carugo *et al.*, 2002). The sites of deduced amino-acid alterations of variant actinin-4 in SCLC were close to those of point mutations in FSGS. Variant actinin-4 protein showed higher affinity to filamentous actin polymers than ubiquitous actinin-4 (Figure 3b), similar to that of mutant actinin-4 in FSGS (Kaplan *et al.*, 2000). As actinin must exist as a head-to-tail dimer to cross-like actin polymers (Djinovic-Carugo *et al.*, 2002), the presence of a small amount of abnormal molecules may affect the overall function of actinin homodimers. In fact, a hemizygous missense mutation of the actinin-4 gene is dominantly inherited in FSGS families (Kaplan *et al.*, 2000). SCLC showed translocation of the entire actinin-4 protein into the nucleus, even in the presence of normal actinin-4 molecules (Figure 1g–i).

In addition to abnormalities of actinin-4, we observed fragility of the actin cytoskeleton to be characteristic of SCLC (Figure 1g–i). Dysregulation of the actin cytoskeleton appears to be an adequate explanation for small cell size, cell fragility and the aggressive behavior of SCLC. However, the NIH3T3 cells expressing exogenous variant actinin-4 protein showed no evidence of cell collapse or nuclear translocation of actinin-4 (Figure 4d–f), but rather showed intensification of actin stress fibers (Figure 4e and red, Figure 4f). We do not presently know whether the expression of variant actinin-4 protein with different actin binding is a result or a cause of the abnormal actin cytoskeleton of SCLC.

Alternative RNA splicing variants with tumor-specificity may be applied for cancer diagnosis and selective treatment. An accurate differential diagnosis of SCLC from non-SCLC is critical for the selection of therapy against lung cancer. Detection of the variant RNA of actinin-4 might provide a good diagnostic marker for SCLC patients.

Expression of the variant actinin-4 was essentially limited to SCLC and testis. Recently, a large number of autoantigens recognized by the host immune system in cancer patients were found to be molecules expressed exclusively in malignant tissues and the testis. These

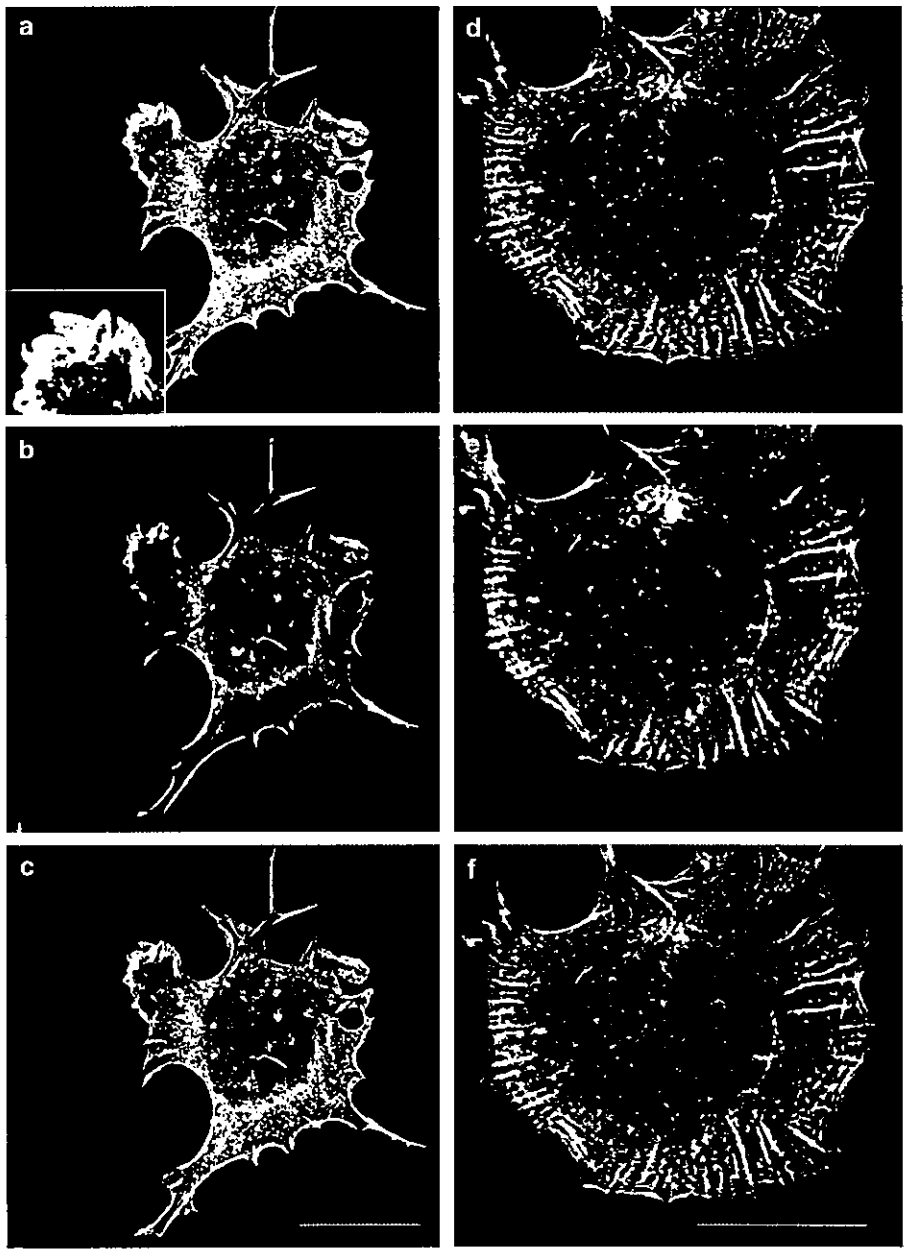

Figure 4 Confocal fluorescence microscopy showing different subcellular localizations of actinin-4 proteins. cDNA fragments of both types of actinin-4 (encoding amino acids 28–911) were amplified by PCR and subcloned into pEGFP-C1 (Clonetech, Palo Alto, CA, USA). NIH3T3 cells were transiently transfected to express EGFP-fusion proteins of ubiquitous (**a**–**c**) and variant (**d**–**f**) actinin-4 using Lipofectamine 2000 (Invitrogen), grown on poly-L-lysin-coated coverslips (Iwaki, Tokyo, Japan) for 36 h, fixed with 4% paraformaldehyde and permeabilized with 0.2% Triton X-100. After staining with Alexa Flour 594 phalloidin (Molecular Probes), coverslips were inspected with a confocal microscope (Radiance 2000MP, BioRad). The images of each EGFP-actinin-4 protein (**a** and **d**) and filamentous actin (**b** and **e**) are merged in (**c**) and (**f**) (actinin-4 in green and actin in red). Bars, 20 μm

so-called CT antigens (cancer-testis antigens) have been recognized as good candidate targets for cancer immunotherapy, because the testis is naturally protected from cytotoxic T lymphocytes (CTL) (dos Santos *et al.*, 2000). Several CT antigens are currently being tested as tumor vaccines in clinical trials (Jager *et al.*, 1999). Recently, Echchakir *et al.* identified an antigen, which was specifically recognized by an autologous tumor-specific CTL clone derived from mononuclear cells infiltrating the primary non-SCLC, as a mutated form of actinin-4. The patient showed a favorable clinical course, probably because of the active immune response against autologous tumor cells expressing the mutant actinin-4 (Echchakir *et al.*, 2001). Variant actinin-4 is a potential target molecule for immunotherapy against SCLC.

Acknowledgements
This study was supported by grants from the Ministry of Health, Labor and Welfare and by the Program for Promotion of Fundamental Studies in Health Sciences of the Organization for Pharmaceutical Safety and Research of Japan.

References

Araki N, Hatae T, Yamada T and Hirohashi S. (2000). *J. Cell Sci.*, **113**, 3329–3340.

Arora VK, Singh N, Chaturvedi S and Bhatia A. (2003). *Acta Cytol.*, **47**, 216–220.

Behrens J, Frixen U, Schipper J, Weidner M and Birchmeier W. (1992). *Semin. Cell Biol.*, **3**, 169–178.

Carney DN, Gazdar AF, Nau M and Minna JD. (1985). *Semin. Oncol.*, **3**, 289–303.

Djinovic-Carugo K, Gautel M, Ylanne J and Young P. (2002). *FEBS Lett.*, **513**, 119–123.

dos Santos NR, Torensma R, de Vries TJ, Schreurs MW, de Bruijn DR, Kater-Baats E, Ruiter DJ, Adema GJ, van Muijen GN and van Kessel AG. (2000). *Cancer Res.*, **60**, 1654–1662.

Echchakir H, Mami-Chouaib F, Vergnon I, Baurain J, Karanikas V, Chouaib S and Coulie PG. (2001). *Cancer Res.*, **61**, 4078–4083.

Hirohashi S and Kanai Y. (2003). *Cancer Sci.*, **94**, 575–581.

Honda K, Yamada T, Endo R, Ino Y, Gotoh M, Tsuda H, Yamada Y, Chiba H and Hirohashi S. (1998). *J. Cell Biol.*, **140**, 1383–1393.

Jager E, Jager D and Knuth A. (1999). *Cancer Metastasis Rev.*, **18**, 143–150.

Kaplan JM, Kim SH, North KN, Rennke H, Correia LA, Tong HQ, Mathis BJ, Rorriguez-Perez JC, Allen PG, Beggs AH and Pollak MR. (2000). *Nat. Genet.*, **24**, 251–256.

Levi F, La Vecchia C, Lucchini F and Negri E. (1996). *Eur. J. Cancer*, **32A**, 652–672.

Michaud JL, Lemieux LI, Dube M, Vanderhyden BC, Robertson SJ and Kennedy CR. (2003). *J. Am. Soc. Nephrol.*, **5**, 1200–1211.

Nikolopoulos SN, Spengler BA, Kisselbach K, Evans AE, Biedler JL and Ross RA. (2000). *Oncogene*, **19**, 380–386.

Shimosato Y, Nakajima T, Hirohashi S, Morinaga S, Terasaki T, Yamaguchi K, Saijo N and Suemasu K. (1986). *Cancer Lett.*, **33**, 241–258.

Small JV, Rottner K and Kaverina I. (1999). *Curr. Opin. Cell Biol.*, **11**, 54–60.

Cell Death and Differentiation (2004) 11, 645–654

www.nature.com/cdd

Regulation of DNaseY activity by actinin-α4 during apoptosis

QY Liu*[,1], JX Lei[1], J LeBlanc[1], C Sodja[1], D Ly[1], C Charlebois[1], PR Walker[1], T Yamada[2], S Hirohashi[2] and M Sikorska*[,1]

[1] Apoptosis Research Group, Institute for Biological Sciences, National Research Council of Canada, Ottawa, Ontario K1A 0R6
[2] Pathology Division, National Cancer Centre Research Institute, 5-1-1 Tsukiji, Chuo-ku, Tokyo, 104-0045, Japan
* Corresponding author: QY Liu and M Sikorska, Neurobiology Program, Institute for Biological Sciences, National Research Council of Canada, 1200 Montreal Rd., Bldg. M-54, Ottawa, Ontario K1A 0R6. Tel: +1 613 990 0850 or +1 613 993 5916; Fax: +1 613 990 7963; E-mail: qing_yan.liu@nrc.gc.ca

Received 08.9.03; revised 11.12.03; accepted 22.12.03; published online 27.02.04
Edited by RA Lockshin

Abstract

DNaseY, a Ca^{2+}- and Mg^{2+}-dependent endonuclease, has been implicated in apoptotic DNA degradation; however, the molecular mechanisms controlling its involvement in this process have not been fully elucidated. We have obtained evidence from yeast two-hybrid screening and coimmunoprecipitation experiments that DNaseY interacted physically with actinin-α4 and this interaction significantly enhanced its endonuclease activity. Accordingly, simultaneous overexpression of both proteins in PC12 cells dramatically increased the rate of apoptosis in response to teniposide' VM26. However, overexpression of DNaseY alone neither triggered apoptosis nor facilitated cell death in response to VM26 or serum deprivation. Instead, the overexpression of DNaseY increased the production of single-strand DNA breaks and evoked a profound upregulation of DNA repair pathways. Taken together, our results point to a novel regulatory mechanism of DNaseY activity and offer an explanation for why cells must first cleave key DNA repair and replication proteins before the successful execution of apoptosis.
Cell Death and Differentiation (2004) **11**, 645–654.
doi:10.1038/sj.cdd.4401401
Published online 27 February 2004

Keywords: actinin-α4; DNA breaks; DNA repair; endonuclease; yeast two hybrid

Abbreviations: MARs, matrix attachment regions; ssb, single-strand break; BUR, base-unpairing region; ds, double strand; ss, single strand; XRCC1, X-ray repair cross complementing 1; Polβ, DNA polymerase β; Lig3, DNA ligase 3; Polδ/ε, DNA polymerase δ/ε; PCNA, proliferating cell nuclear antigen; Lig1, DNA ligase1

Introduction

Progressive DNA cleavage into high molecular weight (HMW) and oligonucleosomal fragments is one of the classical hallmarks of apoptosis. At an early stage of nuclear disassembly, chromatin is cleaved into large domains of 50–300 kilobase pairs (kb). This event has been considered essential for apoptosis and it is, most likely, catalysed by an endonuclease that resides at the matrix attachment regions (MARs) where DNA binds to the nuclear scaffold.[1,2] The second stage of nuclear destruction involves more extensive DNA degradation and usually produces oligonucleosomal DNA ladders. Some authors consider this stage as a housekeeping process, since blocking it does not prevent apoptosis;[3] however, there are also reports arguing that the inhibition of the internucleosomal ladder formation may reduce, or at least delay apoptosis.[4,5] Most apoptotic nucleases characterized to date generate oligonucleosomal DNA fragments; the exceptions are CAD (caspase-3 activated DNase) and DNaseI-like nuclease (DNaseY/DNaseγ in rat, LS-DNase/DNA1IL3 in humans), which have been implicated in both stages of nuclear DNA fragmentation.[6–10]

Multiple mechanisms have been implicated in the activation of endonucleases in apoptosis. For example, some of the enzymes translocate to the nucleus upon receiving an apoptotic signal, that is, endoG from mitochondria and DNaseI from the rough endoplasmic reticulum,[11,12] whereas others, namely L-DNaseII and Helicard, are activated by proteolytic cleavage of their precursors.[13,14] Activation of CAD occurs as a result of proteolysis of its inhibitor ICAD. In proliferating cells, ICAD functions as a CAD-specific chaperone, but upon receiving an apoptotic stimulus, caspases cleave it permitting CAD to degrade chromosomal DNA.[6] Several reports suggest that protease-mediated early degradation of a specific subclass of DNA-binding proteins, such as the base-unpairing region (BUR)-binding proteins, increases the accessibility of endonuclease(s) to these conformationally unstable DNA sequences. This results in the generation of single-strand breaks (ssb) and, subsequently, double-strand (ds) DNA fragmentation.[15–17] Recent reports imply that DNaseY is activated by an increase of intracellular Ca^{2+}, which results in early DNA breaks and activation of PARP-1. Poly-ADP-ribosylation of DNaseY by PARP-1 inhibits its endonuclease activity. This negative regulation of DNaseY may be reversed upon the cleavage and inactivation of PARP-1 by a caspase-3 like protease, followed by reactivation of DNaseY by PAR glycohydrolase.[18,19]

PARP-1 has long been considered a molecular 'nick sensor' that is activated at the sites of ssb and synthesizes negatively charged poly-ADP-ribose.[20–22] Its physical interaction with the base excision repair protein, X-ray repair cross complementing 1 (XRCC1), confirms that PARP-1 is a member of a multiprotein complex involved in the DNA polymerase β, XRCC1 and DNA ligase 3 (Polβ–XRCC1–Lig3) repair pathway.[23] This pathway repairs 50–80% of ssb in living cells.[24] An alternative pathway of ssb repair involves DNA polymerase δ/ε, proliferating cell nuclear antigen and DNA ligase1 (Polδ/ε–PCNA–Lig1 pathway). This pathway conducts ssb repair primarily during DNA replication.

The present study was designed to further investigate the molecular mechanisms controlling the involvement of DNaseY in apoptosis and to examine the effects of conditional overexpression of DNaseY in rat adrenal phaeochromocytoma PC12 cells. We have identified an interaction, both *in vitro* and *in vivo*, between DNaseY and actinin-α4, which resulted in a significant enhancement of DNaseY activity and have shown that concurrent overexpression of both DNaseY and actinin-α4 in PC12 cells significantly accelerated the rate of apoptosis after exposure to teniposide (VM26). Our data also revealed that the overexpression of DNaseY alone was not sufficient to trigger cell death resulting, instead, in the generation of single-strand (ss) DNA breaks and activation of the DNA repair processes that enabled cellular survival.

Results

We have previously shown that DNaseY is constitutively present in mammalian cell nuclei in tight association with chromatin;[8] therefore, it was expected that such a nuclease would be strictly regulated to protect the integrity of DNA. We used yeast two-hybrid screening to search for DNaseY regulatory factor(s). Yeast strain AH109 harbouring the two-hybrid construct (pGBKT7- DNaseY) expressing human DNaseY was used to screen a human brain cDNA library for genes encoding interacting proteins (Figure 1). From 5.3×10^6 transformants, only one clone, displaying Ade/His prototrophy and β-galactosidase activity, was obtained (Figure 1). Sequence analysis and GenBank searches revealed that this clone represented a cDNA encoding the C-terminal fragment of human actinin-α4 (amino acids 448–781), a non-muscle actin-binding protein.[25] The interaction between these two proteins was reproducibly reconstructed in the yeast two-hybrid system and it passed all required specificity tests (Figure 1b).

We then proceeded to establish a cellular model to further characterize the functional relationship between actinin-α4 and DNaseY. Since the endogenous level of DNaseY is very low,[8] we generated stable clones with conditional regulation of DNaseY expression. The DNaseY cDNA was inserted into a bidirectional biEGFP vector and transfected into the commercially available PC12 Tet-on cell line. The endogenous level of DNaseY in this cell line was indeed very low, as shown by both RT-PCR (Figure 2a, lane 1) and Western blotting (Figure 2b, lane 1), hence these cells were considered appropriate for the overexpression studies. Several stable clones were established and shown to produce very high levels of the DNaseY transcript (Figure 2a), particularly in the presence of Dox, but

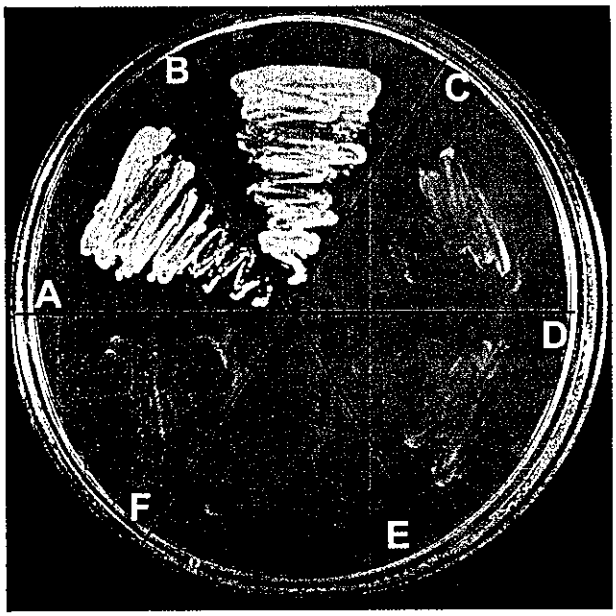

Figure 1 Interaction between DNaseY and actinin-α4 in yeast two-hybrid system. Empty or DNaseY containing pGBKT7 bait vector and empty or actinin-α4 containing pACT2 library vector were cotransformed into yeast host cells AH109 and plated onto SD/-Trp-Leu-Ade-His + X-α-gal plate. (a) A standard positive test showing the interaction between p53 and T antigen; (b) a positive test showing the interaction between DNaseY and actinin-α4; (c) a negative test showing no interaction between lamin C and empty library vector; (d) a negative test of empty bait vector and actinin-α4; (e) a negative test of DNaseY bait vector plus empty library vector; (f) a negative test of empty bait vector plus empty library vector

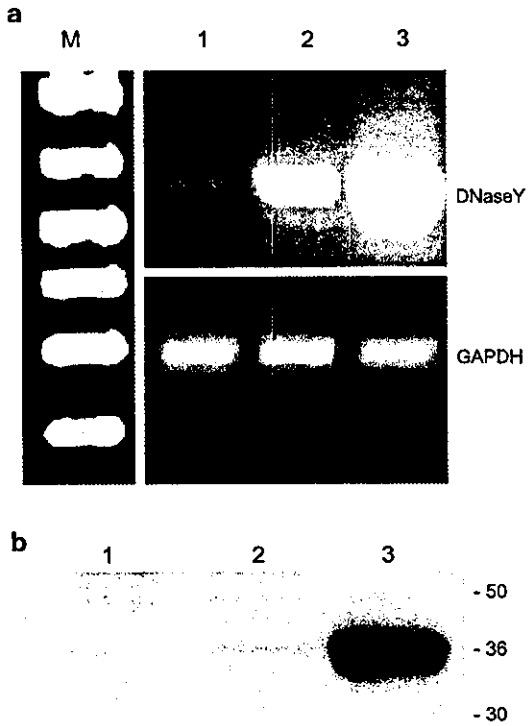

Figure 2 Dox-inducible overexpression of DNaseY in PC12 cells. The PC12 Tet-on cells were stably transfected with DNaseY/biEGFP or empty biEGFP vectors and cultured for 2 weeks in the presence or absence of 1 μg/ml of Dox. The cells were harvested, total cellular RNA and proteins were extracted and analysed by a semi-quantitative RT-PCR (a) and Western blotting (b) as described in Materials and Methods. (a) Ethidium bromide-stained agarose gel of RT-PCR products of DNaseY and GAPDH: lane 1 – cells transfected with empty biEGFP; lane 2 – cells transfected with DNaseY/biEGFP but not exposed to Dox; lane 3 – cells transfected with DNaseY/biEGFP and treated with Dox for 2 weeks (clone 7); M – size markers. (b) Western blot analysis of DNaseY gene product. Equal amounts of total cellular protein (150 μg/lane) were separated on 10% SDS-PAGE, electrotransferred onto a membrane and immunoblotted with anti-DNaseY antibody. Lanes 1–3 represent the same samples as in (a)

even in its absence (due to promoter leakiness). Similar differences were evident at the protein level (Figure 2b).

Nuclear colocalization of DNaseY and actinin-α4 was established based on immunofluorescence staining with specific antibodies (Figure 3). Confocal microscopy revealed that the DNaseY protein was localized mainly in the nuclei of overexpressing cells, although some cytoplasmic staining was also observed (Figure 3a). Actinin-α4, on the other hand, was localized predominantly in the cytoplasmic compartment, likely in the association with the cytoskeleton (Figure 3b). However, a punctuate nuclear immunostaining, indicative of the presence of actinin-α4-positive microdomains was also observed throughout the nucleus. The nuclear presence of actinin-α4 was further confirmed by Western blotting of nuclear protein extracts from the nuclei that were extensively washed and passed through a 2M-sucrose cushion. Based on both the fluorescence (Figure 3c) and phase-contrast (Figure 3d) images, the isolated nuclei were intact, free of cytoskeletal contamination and extracts from these nuclei clearly contained actinin-α4 (Figure 3e, lane 1). This established that DNaseY and a portion of actinin-α4 resided in the nucleus. The protein extract from DNaseY-overexpressing cells (Figure 3f, lane 1) was subsequently used to demonstrate an *in vivo* physical interaction between the two proteins. Immunoprecipitation was performed with anti-actinin-α4 antibody and the Western blot was developed with anti-DNaseY antibody. The blot clearly revealed the presence of DNaseY in the immunoprecipitates (Figure 3f, lane 2).

To determine the biological significance of this interaction, we assessed the effects of actinin-α4 on DNaseY activity *in vitro*. The assay was performed using recombinant His-tag proteins and circular plasmid DNA as a substrate (Figure 4).

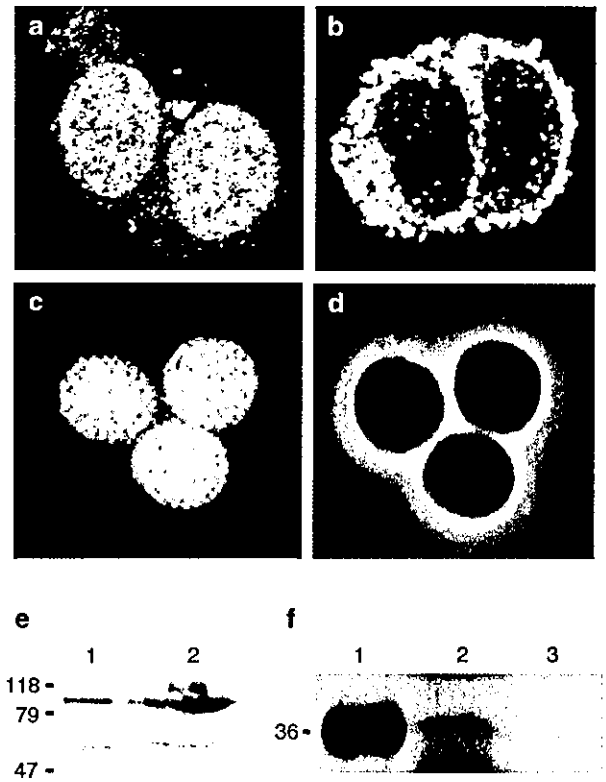

Figure 3 Nuclear colocalization and physical interaction between DNaseY and actinin-α4. (**a, b**) The DNaseY-overexpressing clone 7 was treated with Dox for 2 weeks. The cells were plated on glass coverslips, fixed and immunostained with anti-DNaseY (**a**) and anti-actinin-α4 (**b**) antibodies. The cells were examined and photographed under a Zeiss confocal microscope. (**c, d**) Nuclei were isolated from the Dox-treated clone 7, washed with cytoskeletal stripping buffer, passed through 2 M sucrose cushion and stained with Hoechst 33258 dye. Images, fluorescence (**c**) and phase contrast (**d**) were captured on an Olympus B max fluorescence microscope. (**e**) Proteins were extracted from Dox-treated cells (lane 2) and from isolated nuclei (lane 1), separated on 10% SDS-PAGE (150 μg/lane), electrotransferred onto a nitrocellulose membrane and analysed by Western blotting with anti-actinin-α4 antibody. (**f**) Total cellular proteins from Dox-treated clone 7 were extracted and immunoprecipitated with anti-actinin-α4 antibody as described in Materials and Methods. The precipitates were separated on 10% SDS-PAGE, electrotransferred onto a nitrocellulose membrane and analysed by Western blotting with anti-DNaseY antibody. Lane 1 – total cellular proteins from Dox-treated clone 7; lane 2 – proteins immunoprecipitated with anti-actinin-α4 antibody; lane 3 – mock immunoprecipitation in the absence of primary actinin-α4 antibody

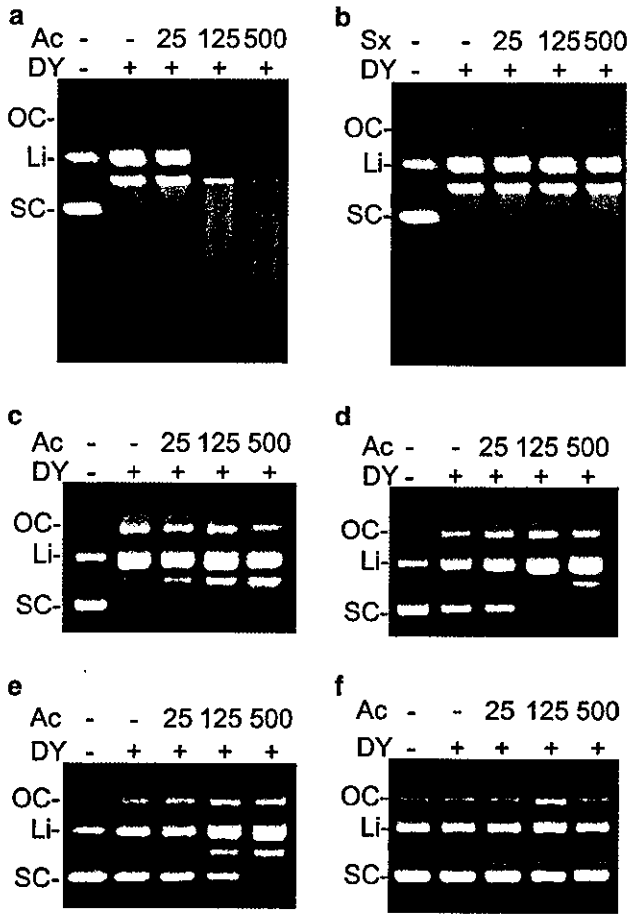

Figure 4 *In vitro* modulation of DNaseY activity by actinin-α4. Increasing amounts of recombinant His-tag actinin-α4 protein (0, 25, 125 and 500 ng, reconstituted in 20 mM Tris-HCl, pH 7.4) were combined with 1 μg of plasmid DNA and preincubated for 30 min at 37°C. An amount of 300 ng recombinant His-tag DNaseY was added to the reactions and incubated for the additional 60 min at 37°C. (**a**) Plasmid digestion was carried out in a 20 μl reaction buffer containing 20 mM Tris-HCl pH 7.4, 5 mM $MgCl_2$ and 2 mM $CaCl_2$; (**b**) the same as in (**a**) except that actinin-α4 was replaced with His-tag Sox2 protein; (**c**) the same as in (**a**) but without $CaCl_2$; (**d**) the same as in (**c**) plus 2 mM EGTA; (**e**) the same as in (**a**) but without $MgCl_2$; (**f**) plasmid digestion was carried out in 20 mM Tris-HCl pH 7.4 in the absence of both $CaCl_2$ and $MgCl_2$. Abbreviations: OC – open circle plasmid; Li – linear plasmid; SC – super coil plasmid. Ac – actinin α4; DY – DNaseY; Sx – Sox2

We have shown previously that DNaseY is optimally active in the presence of Ca^{2+} and Mg^{2+} ions and is capable of single- and double-stranded DNA cleavage.[8] In the reconstituted *in vitro* DNaseY activity assay, performed in the presence of both divalent cations, actinin-α4 significantly accelerated, in a concentration-dependent manner, the digestion of circular plasmid DNA (Figure 4a). This effect was actinin-α4-specific, since a recombinant Sox2 protein, produced and purified in the same fashion as actinin-α4, had no effect on the DNaseY activity (Figure 4b). The concentration-dependent actinin-α4 enhancement of nuclease activity was also seen in assays containing only one cation, that is, Mg^{2+} only (Figure 4c and d) or Ca^{2+} only (Figure 4e), although under such conditions the enzyme was far less active. This was especially true when Ca^{2+} ions were chelated by the addition of 2 mM EGTA (Figure 4d). However, in the absence of both cations actinin-α4 failed to activate DNaseY (Figure 4f). Taken together, these results showed that actinin-α4 could stimulate DNaseY activity at low concentrations of divalent cations, but not in their absence.

Recently, Shiokawa and Tanuma[9] reported that overexpression of DNaseY/DNaseγ in HeLa S3 cells increased the proportion of apoptotic cells in response to C2-ceramide. This assessment was based on morphological changes. We also tested the sensitivity of DNaseY-overexpressing PC12 cells to different apoptosis inducing treatments, that is, the topoisomerase II inhibitor teniposide (VM26) and deprivation of growth factors (Figure 5). Several clones were selected, cultured for 2 weeks in the presence of Dox to achieve maximal induction of DNaseY expression (Figure 2) and subsequently treated for 24 h with 10 μM VM26 (Figure 5a). Approximately 40–50% of cells lost viability as a result of this treatment; however, the overexpression of DNaseY, clearly, had no effect on the rate of cell death in response to VM26. Similar behaviour was observed after a 24 h period of serum withdrawal (Figure 5b). None of the overexpressing clones showed higher sensitivity than control cells carrying empty vectors. The DNA degradation pattern in response to VM26 treatment was analysed by PFGE and is shown in Figure 6. These cells did not produce oligonucleosomal ladders; instead, the DNA was cleaved into a range of large fragments of 300 kb and above as well as 50 kb and below (Figure 6). Similar results were obtained with other treatments (data not shown). Taken together, these results indicated that the overexpression of DNaseY by itself neither triggered apoptotic cell death nor accelerated it in response to the well-known triggers, that is, VM26 and serum deprivation.

The lack of sensitivity of the overexpressing cells contradicted the previously published reports[9] and raised a question of whether the clones were actually expressing active DNaseY enzyme. To address this, we isolated the nuclei and examined *in vitro* chromatin digestion during a 60 min incubation period (Figure 7). After the incubation, the nuclei were embedded in agarose plugs and DNA integrity was assessed by PFGE.[26] A comparison was made between the nuclei obtained from cells carrying empty biEGFP vector and from cells containing the vector encoding DNaseY. Prior to isolation of the nuclei, the cells were cultured for 2 weeks with Dox to achieve full induction of DNaseY expression. There was no DNA degradation in the absence of divalent cations,

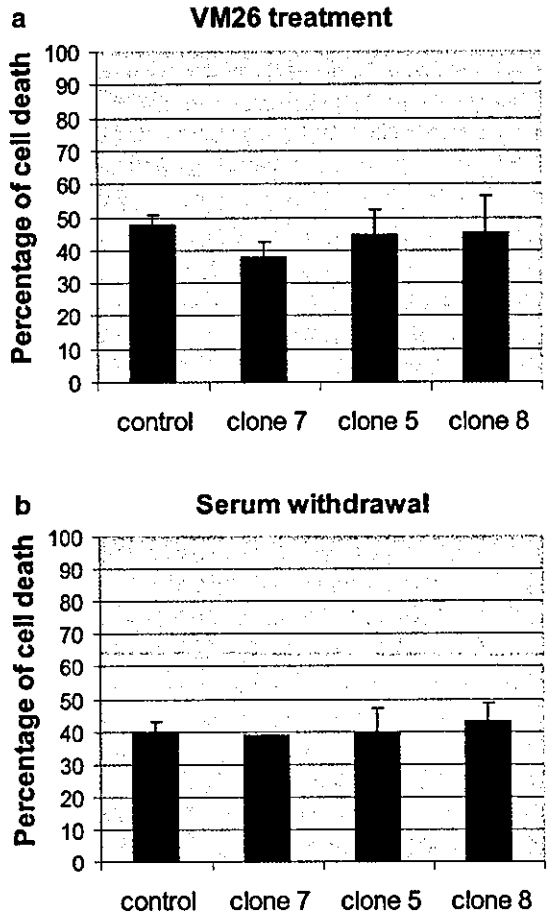

Figure 5 Induction of apoptosis in DNaseY-transfected clones. The PC12 Tet-on cells carrying empty biEGFP vector (control) and cells transfected with DNaseY/biEGFP (clones 5, 7 and 8) were cultured for 2 weeks in the presence of 1 μg/ml of Dox. Cell death was induced by a 24 h exposure to either 10 μM VM26 (**a**) or serum withdrawal (**b**). Cell viability was assessed by counting trypan blue positive cells using a haemocytometer

regardless of whether the cells expressed DNaseY or not (Figure 7, lanes 6–9). In the presence of Mg^{2+} ions, there was a significant difference between the control and overexpressing clones (Figure 7, compare lanes 10 and 11 to lanes 12 and 13), especially after the Dox treatment when the entire nuclear DNA content was converted to oligonucleosomal ladders (Figure 7, lane 13). More extensive chromatin digestion was observed during incubation with both Ca^{2+} and Mg^{2+} (Figure 7, lanes 14–17), especially in nuclei from the overexpressing cells in which DNA digestion neared completion (Figure 7, lanes 16 and 17). These results showed that DNaseY was active and capable of efficient chromatin fragmentation in isolated nuclei. Yet, in the context of the intact cell, its presence did not accelerate apoptosis.

Thus far, we have established that actinin-α4 was capable of modulating DNaseY activity *in vitro* (Figure 4). To test their interaction *in vivo*, we transiently transfected a pcDNA 3.1/Myc-His plasmid harbouring full-length human actinin-α4 cDNA into the control and DNaseY-overexpressing cells and challenged the cells with either 10 μM VM26 or 1 μM staurosporine for 24 h (Figure 8). Again, in the absence of

Figure 6 Analysis of DNA fragmentation by PFGE. Control PC12 Tet-on cells with empty biEGFP vector and DNAseY overexpression clone 7 were cultured for 2 weeks in the presence of 1 μg/ml of Dox. Apoptosis was induced by the 24 h treatment with 10 μM VM26. Equal numbers of cells were embedded in LMP agarose plugs and analysed by PFGE as described in Materials and Methods. The gel was stained with ethidium bromide and photographed on a transilluminator. Lane 1 – control untreated cells; lane 2 – clone 7 untreated; lane 3 – control cells treated with VM26; lane 4 – clone 7 treated with VM26. The size markers were: 123 bp DNA ladder; low range PFG marker (λ DNA - *Hind* III fragments); ladder PFG marker; yeast chromosome PFG marker (*S. cerevisiae* YPH 80)

exogenous actinin-α4, the response of the DNaseY-overexpressing clone was the same as the empty vector control (approximately 40% of cells lost membrane integrity and became trypan blue positive). The expression of actinin-α4 in control cells also had no effect on their sensitivity to VM26. However, the picture was vastly different after the introduction of actinin-α4 into the DNaseY-overexpressing cells; the rate of cell death doubled and, within 24 h, approximately 70% of cells were dead (Figure 8). The cells were dying by apoptosis as evidenced by the characteristic chromatin condensation seen in Hoechst dye-stained nuclei (Figure 8, inset). Similar results were obtained in response to staurosporine (data not shown). These experiments confirmed that actinin-α4 was capable of DNaseY activation *in vivo*.

The question still remained as to why prolonged overexpression of the active endonucleolytic enzyme had no effect on the sensitivity to apoptosis? For example, we have treated

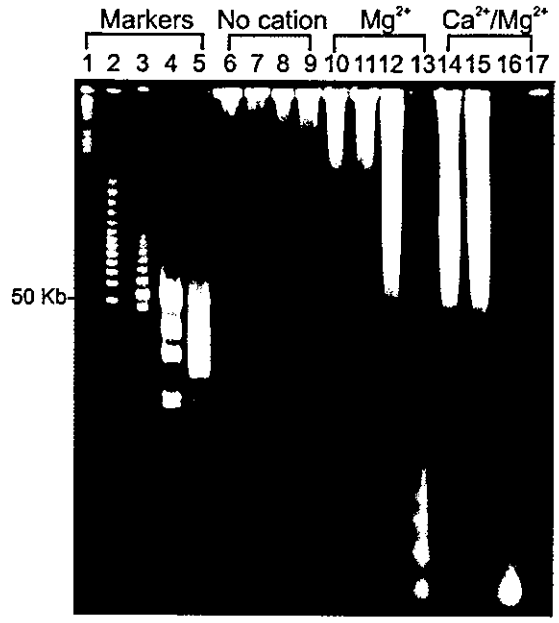

Figure 7 PFGE analysis of DNA fragmentation in isolated nuclei. Isolated nuclei were incubated for 60 min at 37°C in the presence or absence of divalent cations and embedded in LMP agarose plugs. Equal amounts of DNA were loaded onto a 0.8% agarose gel and analysed by PFGE as described in Materials and Methods. The gel was stained with ethidium bromide and photographed on a transilluminator. Lanes 6, 10 and 14 – nuclei from the empty vector control cells not treated with Dox; lanes 7, 11 and 15 – nuclei from control cells cultured for 2 weeks in the presence of 1 μg/ml of Dox; lanes 8, 12 and 16 – nuclei from clone 7 not treated with Dox; lanes 9, 13 and 17 – nuclei from clone 7 treated with Dox for 2 weeks. The molecular size markers used were: yeast chromosome PFG marker (*S. cerevisiae* YPH 80); λ ladder PFG marker; low range PFG marker (λ DNA - *Hind* III fragments); λ DNA *Hind* III marker; 123 bp DNA ladder

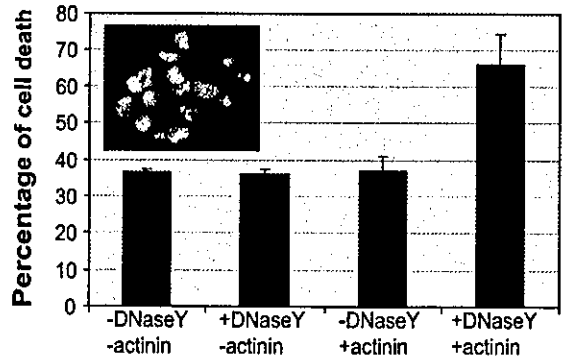

Figure 8 *In vivo* activation of DNaseY by actinin-α4. The empty vector control and DNAseY-overexpressing clone 7 were treated for 2 weeks with 1 μg/ml of Dox and were subsequently transiently transfected with a plasmid encoding the full length actinin-α4 cDNA. After 24 h, the transfected cells were challenged with 10 μM VM26 and cell viability was assessed by trypan blue exclusion assay after the additional 24 h. −DNaseY/−actinin – nontransfected empty vector control; +DNaseY/−actinin – nontransfected clone 7; −DNaseY/+actinin – control cells transfected with actinin-α4 cDNA; +DNaseY/+actinin – clone 7 transfected with actinin-α4. Inset: Cells (clone 7) were exposed to VM26 for 24 h, fixed and stained with Hoechst dye and examined under an Olympus B × 50 fluorescence microscope

the clones with Dox for up to 5 weeks and established that these cells continued to produce very high levels of DNaseY (Figure 2) and, yet, they continued to grow and proliferate and did not change their susceptibility to the apoptotic inducers.

However, while searching for evidence of nuclear DNA degradation, using the terminal deoxynucleotidyl transferase (TdT)-mediated nick end labelling (TUNEL) assay, we discovered that the entire population of DNaseY-overexpressing cells, especially after 2 weeks of induction with Dox, was brightly stained and TUNEL-positive (Figure 9a–c). Without Dox treatment, the intensity of TUNEL staining was much lower (Figure 9d–f). Moreover, the nuclear morphology of these cells was normal, without any evidence of apoptotic chromatin collapse, and the cells continued to grow and proliferate at the same rate as control cells with TUNEL-negative nuclei (Figure 9g–i). In the control cell population, TUNEL-positive nuclei with classical apoptotic morphology were only occasionally seen (Figure 9a–c). Clearly, the overexpression of active DNaseY leads to the generation of extensive DNA breaks with 3′-OH ends recognized and labelled by terminal deoxynucleotidyl transferase employed in the TUNEL assay. This observation raises concerns about the reliability of the TUNEL assay for the detection of early apoptotic cells, as every cell overexpressing DNaseY was TUNEL positive, but had normal nuclear morphology and continued to proliferate (Figure 9g and h).

The presence of ss DNA breaks was further revealed by two-dimensional gel electrophoresis.[27] Although DNA remained in the wells and seemed intact after separation in the first dimension by PFGE (Figure 10, top panel), alkaline denaturation prior to conventional electrophoresis in the second dimension liberated a tail of ss DNA fragments. This was especially evident in Dox-treated DNaseY overexpressing cells (Figure 10, bottom panel). Therefore, to grow, proliferate and faithfully replicate their genetic information, these cells must have an efficient DNA repair system to cope with the unusually high levels of ssb. To test this, we used Western blotting to determine the levels of several components of the DNA repair pathways (Figure 11). Firstly, we found that induction of DNaseY expression caused a significant upregulation of PARP-1, the ssb sensor protein (Figure 11a, lane 3). Secondly, there was also an induction of the Polβ–XRCC1–Lig3 pathway, as manifested by the increased expression of XRCC1 and Lig3 proteins. XRCC1 is the docking scaffold protein that interacts with PARP, PNK, Polβ, and Lig3. As shown in Figure 11b, its upregulation in the DNaseY-overexpressing cells was very significant, as was the elevation of both the 97 and 100 kDa forms of Lig3 (Figure

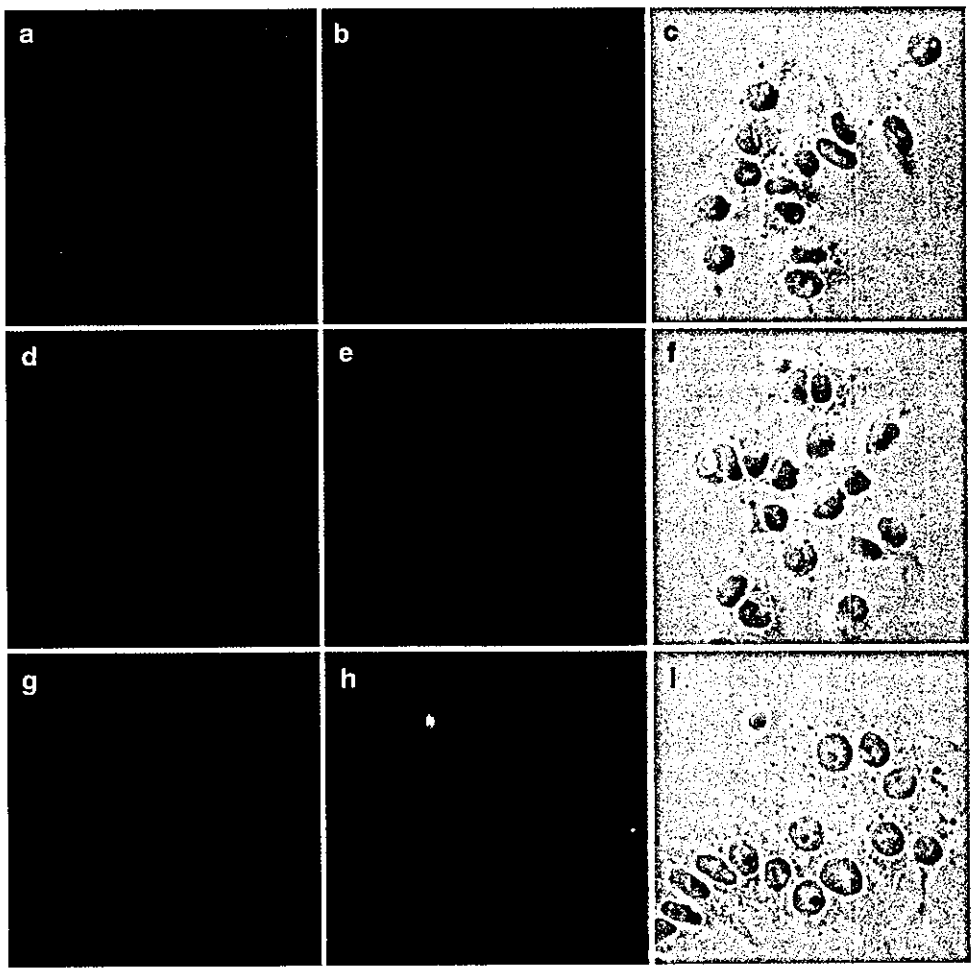

Figure 9 Identification of ss DNA breaks by TUNEL. The DNaseY-overexpressing clone 7 treated (**a–c**) or nontreated (**d–f**) for 2 weeks with Dox and empty vector control cells (**g–i**) were plated on glass coverslips, fixed and labelled with terminal deoxynucleotidyl transferase using biotin-16-dUTP and CY3-conjugated streptavidin (**a, d** and **g**). Nuclei were counterstained with DAPI (**b, e** and **h**). The same cells were also photographed with phase contrast optics (**c, f** and **i**)

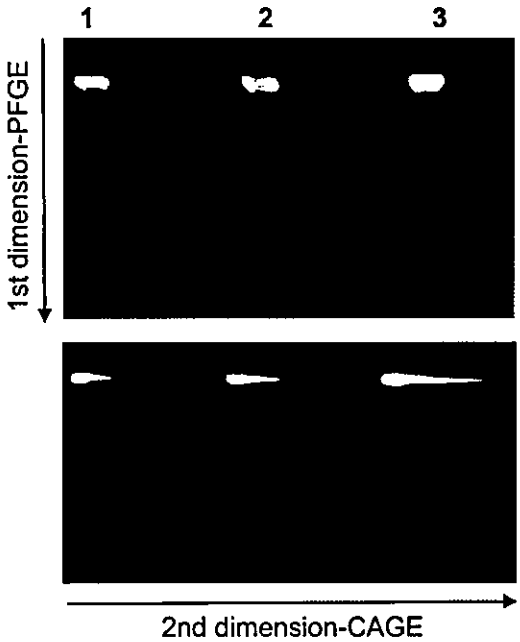

Figure 10 Two-dimensional analysis of DNA fragmentation. DNA from control, DNaseY-overexpressing clone 7 (noninduced and induced by Dox) was processed in agarose plugs and analysed by PFGE in a first dimension (top panel) and by CAGE in a second dimension (bottom panel), as described in Materials and Methods

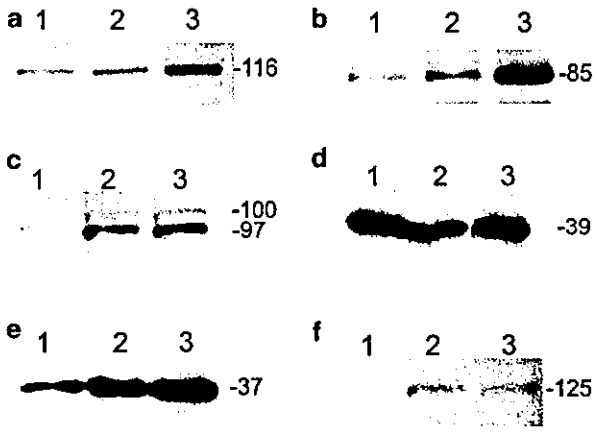

Figure 11 Western blotting analyses of DNA repair components. Nuclei were isolated from the empty vector control cells (lane 1) and from DNaseY-overexpressing clone 7, noninduced (lane 2) and induced by Dox (lane 3), and nuclear proteins were extracted as described in Materials and Methods. Amounts of 50 μg per lane of total nuclear proteins were separated on 10% SDS-PAGE, electrotransferred onto a nitrocellulose membrane and immunoblotted with anti-PARP-1 (a), anti-XRCC1 (b), anti-Lig3 (c), anti-Polβ (d), anti-PCNA (e) and anti-Lig1 (f) antibodies

11c). The expression of Polβ, on the other hand, did not change (Figure 11d). Finally, the expression of two components of the Polδ/ε–PCNA–Lig1 complex, PCNA and Lig1, was also upregulated in the DNaseY-overexpressing cells (Figure 11e and f).

Discussion

This study was undertaken to examine molecular mechanisms controlling the involvement of DNaseY in apoptosis. Previous studies have shown that this nuclease meets most of the biochemical and functional criteria (i.e., cation dependence, pH profile, ability to cleave ss and ds DNA with 3′-OH ends, nuclear localization) expected of an enzyme engaged in the apoptotic process.[8] The constitutive presence of DNaseY in the nucleus suggests that its physiological role might be linked to the maintenance of DNA integrity and that its participation in cell death process must be tightly controlled. We have demonstrated that actinin-α4 protein could modulate DNaseY enzymatic activity both *in vitro* and *in vivo* (Figures 4 and 8). In the *in vitro* assay, actinin-α4 significantly stimulated it, particularly under less than optimal concentration of divalent cations, although not in their absence (Figure 4). This interaction *in vivo* resulted in a highly accelerated rate of cell death in response to apoptotic stimuli (i.e. VM26 and staurosporine, Figure 8).

The molecular mechanisms that govern the interaction and activation of DNaseY by actinin-α4 are at present unknown. Actinin-α4 is one of the four mammalian α-actinin genes, all of which encode highly homologous, approximately 100 kDa actin crosslinking or bundling proteins.[28] These proteins contain a C-terminal EF hand calcium-binding domain and are believed to link the actin cytoskeleton to focal adhesions and control cell motility. Although actinin-α4 is a calcium-binding protein, it did not substitute for the requirements of divalent cations and DNaseY was completely inactive in their absence (Figure 4). However, the *in vivo* data showed that cell death was accelerated only when both proteins were overexpressed simultaneously, implying that the activation process might require formation of a physical complex, which is supported by the results of the coimmunoprecipitation experiments (Figure 3).

We have established that in addition to a prominent cytoplasmic localization, a fraction of actinin-α4 was also present in the nuclei of PC12 cells (Figure 3). These observations are consistent with those of Honda *et al.*,[25] who reported recently that actinin-α4 exists in the nuclei of a certain population of breast cancer cell lines. Furthermore, these authors show that actinin-α4 translocates from the cytoplasm to the nucleus following treatments with wortmannin, the PI3 kinase inhibitor or cytochalasin D, the actin-depolymerizing drug. This translocation alters cellular motility and abolishes the cells' tumorigenic and metastatic potential.[25,29] Although the precise mechanism of nuclear translocation has not been identified (actinin-α4 does not contain any apparent nuclear localization signals), the involvement of PI3 kinase is of great interest. PI3 kinase is one of the key molecules involved in the signalling pathways of activated receptor tyrosine kinases and regulates vital cellular processes (i.e., cell growth, motility, morphogenesis) as well as protecting the cells from apoptosis.[30] Therefore, we may speculate that activation of DNaseY, at least in some cell types, could be brought about by the nuclear translocation of actinin-α4 facilitated by the inactivation of PI3 signalling. This sequence of events is supported by our results. For example, the active nuclease was capable of complete destruction of

nuclear chromatin in the isolated nuclei (Figure 7), but not in intact cells (Figure 5). Thus, only after the removal of cytoplasmic control, or after the introduction of exogenous actinin-α4 (Figure 8), the effect of DNaseY overexpression became evident. It is also possible to speculate that the tumour suppressor function of actinin-α4 might be linked to its ability to stimulate DNaseY and consequently enhance apoptosis of cancer cells.[25,29]

The true physiological function of DNaseY is still not known, although its nuclear presence and close association with chromatin suggests that it plays a role in DNA metabolism. We have demonstrated here, for the first time, that DNaseY produced widespread ss DNA breaks. However, extensive accumulation of ssb (Figure 9) did not push the PC12 cells into apoptosis. This is in agreement with the previous studies, which reported that transfection of the same nuclease into HeLa cells or mouse skin fibroblasts increased cell death only in response to apoptotic stimuli, but not by itself.[9,18] In our cell system, overexpression of DNaseY led to the activation of DNA repair pathways. The components of both repair systems, the Polβ–XRCC1–Lig3 pathway, which conducts both short and long-patch repair as well as the Polδ/ε–PCNA–Lig1 pathway, which provides an alternative or 'backup' mechanism for ssb repair and often conducts long-patch break repair,[24] were clearly upregulated in the DNaseY-overexpressing cells (Figure 11e and f). The expression of Polβ, on the other hand, was not altered (Figure 11d) suggesting that DNaseY generated simple nicks on the DNA strands rather than gaps, which would require the activity of polymerase. Therefore, to fully engage in the execution of apoptosis, the cells must also degrade the key proteins involved in the DNA repair processes.[31]

It has been reported that, at early stages of apoptosis, DNaseY can be inactivated by PARP-1 through the poly-ADP-ribosylation mechanism.[18,19] Here we found a significant upregulation of PARP-1 in the DNaseY-overexpressing cells (Figure 11a). Therefore, it is possible that PARP-1 acts both as a sensor to detect ssb and at the same time to synthesize negatively charged ADP-ribose polymers to inhibit the endonuclease that creates them.[20,32] In the execution phase of apoptosis, PARP-1 is cleaved and inactivated by caspase-like proteases relieving inhibition of DNaseY;[18,19] however, the inactivation of PARP-1 may not be sufficient to fully unleash the activity of DNaseY. The cytoplasmic changes, that is, alterations in signalling pathways and cytoskeletal changes, might also be required to accomplish this.

In conclusion, we have established that DNaseY, a Ca^{2+}- and Mg^{2+}-dependent endonuclease, was capable of producing ss DNA breaks and its activity was modulated by actinin-α4. Moreover, the ssb's produced by exogenous DNaseY were not detrimental to the cells as the cells activated the DNA repair processes to cope with this burden. Although it is still not clear whether, under normal physiological conditions, DNaseY plays a role in DNA repair and/or replication, the accumulated evidence suggests that it does also have a role in apoptosis. Other endonucleases implicated in apoptosis also have regular housekeeping functions. For example, EndoG is a mitochondrial enzyme that plays a role in DNA replication. It becomes involved in apoptotic process only when released from the mitochondria.[11,33] L-DNaseII in its native form is a serine protease inhibitor (LEI); it transforms into a nuclease during apoptosis.[34]

Materials and Methods

Cell culture and experimental treatments

Rat adrenal phaeochromocytoma PC12 Tet-On cell line was purchased from Clontech (Palo Alto, CA, USA). The cells were cultured in Dulbecco's modified Eagle's medium (DMEM) supplemented with 10% horse serum, 5% fetal calf serum (Wisent Inc., St. Bruno, QC), 0.1 mg/ml gentamycin sulphate (Sigma Cell Culture, St. Louis, MO, USA), 230 μg/ml active G418 sulphate (Gibco BRL, Burlington, ON), and 25 μg/ml hygromycin B (Boehringer Mannheim, Montreal, QC). To induce the expression of DNase Y transcripts, cells were cultured in a medium containing 1 μg/ml Doxycycline (DOX, Sigma, Oakville, ON) for 2 weeks prior to the initiation of experiments. Cell death was triggered by either 24 h exposure to 10 μM VM26, 1 μM staurosporine or by serum withdrawal. Cell viability was assessed by the trypan blue exclusion assay using a haemocytometer.

Cell transfections

A fragment of DNase Y cDNA (lacking the N-terminal 25 amino acids encoding the signal peptide) encoding the active DNaseY protein was cloned into the biEGFP vector (Clontech, Palo Alto, CA, USA) and used to generate stable clones with conditional Tet-on regulation of DNaseY expression. The cells were transfected using the Calphos Mammalian transfection kit (Clontech, Palo Alto, CA, USA). Briefly, the PC12 Tet-on cells, cultured for 24 h in 10 cm Petri dishes (2×10^6 cells per dish), were placed in fresh medium 1 h prior to the transfection. Amounts of 10 μg of DNaseY/biEGFP or empty biEGFP vector control along with 2.5 μg of pHeBo were used per Petri dish. The transfection cocktail was prepared by adding the cDNA plasmids and calcium-Maximizer solution to 2 × PBS buffer drop by drop with constant bubbling and a subsequent 15 min incubation at room temperature. A volume of 700 μl of this transfection cocktail was added to each Petri dish. The cells were incubated for 5 h at 37°C, washed once with PBS and placed in 10 ml of fresh complete growth medium. At 72 h post transfection, the cells were trypsinized, split 1:5 and subsequently cultured in growth medium containing 25 μg/ml hygromycin B (Boehringer Mannheim, Germany). Positive colonies were selected using a Zeiss IM35 inverted fluorescence microscope.

Transient transfections of DNaseY-overexpressing cells with a plasmid encoding actinin-α4 were also performed. Full-length human actinin-α4 cDNA was cloned into pcDNA 3.1/Myc-His vector (Invitrogen, Burlington, ON). Cells were plated in 12-well plates (0.4×10^6 cells/well) 1 day before and were transfected with 5 μg/well of purified plasmid harbouring actinin-α4 cDNA and 15 μl of LipofectAmine 200 reagent (Invitrogen, Burlington, ON) according to the manufacturer's instruction.

RNA extraction and RT-PCR

Total RNA extraction, first-stand cDNA synthesis and RT-PCR analysis of DNaseY transcript were performed as previously described.[8]

Antibody production

Rat cDNA encoding an active DNaseY protein was cloned into pBAD/HisA vector (Invitrogen, Burlington, ON). Recombinant His-tag DNaseY protein was purified by His-Trip nickel column (Pharmacia Biotech, Baie d' urfe', QC). The proteins were freeze-dried and reconstituted in PBS for

vaccination. White male New Zealand rabbits were first immunized with 500 μg of protein/inoculation according to standard operating protocol. Animals were boosted three times with 250 μg protein, within a 4-week interval. The titre of the antibody was tested at 10–14 days after each boosting. Polyclonal anti-DNaseY antibody was collected 14 days after the third boosting.

Immunofluorescence staining

Cells were plated on poly-L-lysine-coated coverslip, fixed with paraformaldehyde (J.B. EM Services Inc., Point-Claire, PQ). Fixed cells were immunostained with one of the following primary antibodies diluted in PBS: anti-DNaseY (1 : 300 v/v[8]), or anti-actinin-α4 (1 : 10 v/v[25]). Cells were then incubated for 1 h in the corresponding secondary antibody: Cy3-conjugated goat anti-mouse Ig $G_{(Fc)}$ (1 : 200) or CY3-conjugated goat anti-mouse IgM(μ) (diluted 1 : 200, both from Jackson ImmunoResearch/BioCan Scientific, Mississauga, ON). Finally, the nuclei were counterstained with 0.2 μg/ml of 4′, 6-diamidino-2-phenylindole (DAPI) or Hoechst 33258 (Sigma, Oakville, ON) in PBS for 5 min and were mounted in Vectashield mounting medium (Vector Laboratories Inc., Burlingame, CA, USA). Optical sections were obtained on a Zeiss LSM-410 (Carl Zeiss, Thornwood, NY, USA) inverted laser scanning microscope equipped with a krypton/argon laser. CY3-labelled cells were analysed using a 530–585 nm-band pass filter and dichroic mirror (FT 488/568) for excitation, and a 575–640 nm-band pass filter to detect emission.

DNA breaks were detected by TUNEL essentially performed as described by Gavrieli *et al.*[35] using biotin-16-dUTP (Boehringer Mannheim, Laval, PQ) and visualized with CY3-conjugated streptavidin (Jackson ImmunoResearch, West Grove, PA, USA). The cells were examined on an Olympus B max fluorescence microscope with Olympus × 40 N.A. 1.0 planapo oil immersion objective and images were processed using Northern Exposure software and Adobe Photoshop 5.5.

Protein extraction

Total cellular and nuclear proteins were extracted as described by Liu *et al.*[17] The cytoskeletal structures were removed from the nuclear pellet by washing with cytoskeletal stripping buffer (BNB buffer containing a 2 : 1 ratio (v/v) of NP-40 and sodium deoxycholate in a final concentration of 1% : 0.5%) for 15 min and centrifugation at 3000 r.p.m. for 5 min at 4°C. To ensure total removal of any cytoplasmic protein, the nuclei were resuspended in 300 μl of BNB, mixed with 3 ml sucrose cushion buffer (50 mM Tris-HCl, pH 7.4, 2 M sucrose, 5 mM $MgCl_2$) and loaded on a top of 1 ml sucrose cushion buffer in a 5 ml ultracentrifuge tube. After centrifugation at 13 000 r.p.m. for 1 h, the nuclear pellet was further washed with fresh BNB buffer and a small sample was examined under the microscope to check for cytoplasmic protein contamination. The nuclei were finally collected by centrifugation at 3000 r.p.m. for 5 min at 4°C. The pellet was resuspended in a buffer containing 20 mM HEPES, pH 7.9, 420 mM NaCl, 25% glycerol, 0.2 mM EDTA, 1.5 mM $MgCl_2$, 0.5 mM DTT and 0.5 mM PMSF and incubated on ice for 30 min. The nuclear proteins were collected either by ultracentrifugation at 55 000 r.p.m. at 4°C for 10 min, or by direct sonication on ice for 10 × 5 s.

Western blotting

Immunoblottings were performed as previously described.[8] The blots were probed with the following primary antibodies: rabbit polyclonal anti-DNaseY (dilution 1 : 1000), mouse monoclonal anti-DNA ligase III (1 : 200 v/v, Genetex, San Diego, CA, USA), mouse monoclonal anti-XRCC1 (1 : 1000 v/v, Trevigen, Gaithersburg, MD, USA), mouse monoclonal anti-DNA ligase I (1 : 200 v/v, QED Biosciences Inc, San Diego, CA, USA), mouse monoclonal anti-PCNA (1 : 200 v/v, Calbiochem, Hornby, ON), mouse monoclonal anti-DNA polymerase β (1 : 100 v/v, NeoMarker, Fremont, CA, USA), mouse monoclonal anti-PARP (1 : 5000 v/v, Upstate Biotechnology, Charlottesville, VA, USA) and mouse monoclonal anti-actinin-α4 (1 : 10 v/v[25]). The antigens were detected using horseradish peroxidase-conjugated secondary antibodies: goat anti-mouse IgG (1 : 5000 v/v), donkey anti-rabbit IgG (1 : 5000 v/v, both from Promega Corporation, Madison, WI, USA), goat anti-mouse IgM (1 : 5000 v/v, Jackson ImmunoResearch, West Grove, PA, USA) and the complexes were revealed by enhanced chemiluminescence using the ECL kit (Amersham Biosciences, Baie d' urfe', PQ, Canada).

Coimmunoprecipitation

Magnetic Dynabeads (Dynal Biotech Inc.,. Lake Success, NY, USA) were prepared by resuspending 20 μl of beads in 500 μl of Co-IP buffer (20 mM Tris–HCl, pH 7.5, 150 mM NaCl, 0.1% Tween–20, 0.1% BSA, 1 × protease inhibitor cocktail), mixing on a rotator for 2 min, then recovering the beads with a magnetic stand. This step was repeated three times. The beads were then mixed with 500 μl Co-IP buffer and 2 μl anti-mouse IgM conjugated with biotin (Jackson ImmunoResearch, West Grove, PA, USA) for 30 min, recovered, washed five times with Co-IP buffer, then blocked in 500 μl Co-IP buffer with 0.5% BSA for 30 min on a rotator. The beads were again recovered and washed twice with Co-IP buffer. The sample protein was cleaned by mixing 500 μg to 1 mg with the beads in 100 μl Co-IP buffer for 1 h at 4°C. The beads were discarded; the protein was recovered and mixed with 5 μl of mouse monoclonal anti-actinin-α4 antibody[25] for 2 h at 4°C. This mixture was added to a fresh set of beads, prepared as described above, and mixed overnight at 4°C. The beads were recovered, washed three times with Co-IP buffer without BSA. The bead-bound complexes were released by boiling in protein loading buffer for 5 min. The presence of DNaseY in the complex was revealed by Western blotting as described above.

Analysis of DNA fragmentation

Nuclei auto-digestion was carried out as described in Pandey *et al.*[26] Conventional, pulsed field and two-dimensional gel electrophoresis of DNA was performed exactly as previously described.[27]

Yeast two-hybrid screening

Human DNaseY cDNA encoding the active DNaseY protein was cloned into pGBKT7 vector (Clontech, Palo Alto, CA, USA) to generate a chimaeric open reading frame encoding Gal4 DNA binding domain and DNaseY protein. This construct was introduced into yeast *Saccharomyces cerevisiae* strain AH109. A single colony containing cells harbouring the DNaseY/pGBKT7 plasmid was then used as host cells for screening a human cDNA expression library constructed in pACT2 vector (Clotech, Palo Alto, CA, USA). The protein–protein interaction was first screened by plating the transformants onto SD/-Trp-Leu-His-Ade selection plates. Positive clones were then rescreened for the presence of β-galactosidase activity to eliminate false-positive interaction. Library plasmids harbouring DNaseY interacting proteins were rescued and reintroduced into the DNaseY/pGBKT7 containing host cell to further eliminate false interaction. The identity of the cDNA encoding DNaseY-interacting protein was revealed by DNA sequencing and database searches.

DNase Y activity assay

The activity assay was performed by preincubation of 1 μg of plasmid DNA with variable amounts of purified His-tag human actinin-α4 protein in 20 μl buffer containing 20 mM Tris-HCl, pH 7.4, 5 mM $MgCl_2$ and 2 mM $CaCl_2$ for 30 min at 37°C. A volume of 5 μl (0.3 μg) purified His-tag rat DNaseY was then added to the reaction and incubated for 60 min at 37°C. The pattern of plasmid DNA digestion was analysed by electrophoresis on 0.8% agarose gels in 40 mM Tris-acetate buffer pH 8.5 and 2 mM EDTA at 20 V overnight. Gels were stained with ethidium bromide and photographed on a UV transilluminator, and analysed by agarose gel electrophoresis in TAE buffer.

Acknowledgements

We thank Joanne Chartier and Min Wang for their technical assistance.

References

1. Lagarkova MA, Iarovaia OV and Razin SV (1995) Large-scale fragmentation of mammalian DNA in the course of apoptosis proceeds via excision of chromosomal DNA loops and their oligomers. J. Biol. Chem. 270: 20239–20241
2. Walker PR and Sikorska M (1997) New aspects of the mechanism of DNA fragmentation in apoptosis. Biochem. Cell Biol. 75: 287–299
3. Sakahira H, Enari M and Nagata S (1998) Cleavage of CAD inhibitor in CAD activation and DNA degradation during apoptosis. Nature 391: 96–99
4. Walisser JA and Thies RL (1999) Poly(ADP-ribose) polymerase inhibition in oxidant-stressed endothelial cells prevents oncosis and permits caspase activation and apoptosis. Exp. Cell Res. 251: 401–413
5. Boulares AH, Zoltoski AJ, Sherif ZA, Yakovlev AG and Smulson ME (2002) The Poly(ADP-ribose) polymerase-1-regulated endonuclease DNAS1L3 is required for etoposide-induced internucleosomal DNA fragmentation and increases etoposide cytotoxicity in transfected osteosarcoma cells. Cancer Res. 62: 4439–4444
6. Enari M, Sakahira H, Yokoyama H, Okawa K, Iwamatsu A and Nagata S (1998) A caspase-activated DNase that degrades DNA during apoptosis, and its inhibitor ICAD. Nature 391: 43–50
7. Baron WF, Pan CQ, Spencer SA, Ryan AM, Lazarus RA and Baker KP (1998) Cloning and characterization of an actin-resistant DNase I-like endonuclease secreted by macrophages. Gene 215: 291–301
8. Liu QY, Pandey S, Singh RK, Lin W, Ribecco M, Borowy-Borowski H, Smith B, LeBlanc J, Walker PR and Sikorska M (1998) DNaseY: a rat DNaseI-like gene coding for a constitutively expressed chromatin-bound endonuclease. Biochemistry 37: 10134–10143
9. Shiokawa D and Tanuma S (1998) Molecular cloning and expression of a cDNA encoding an apoptotic endonuclease DNase gamma. Biochem. J. 332: 713–720
10. Yakovlev AG, Wang G, Stoica BA, Simbulan-Rosenthal CM, Yoshihara K and Smulson ME (1999) Role of DNAS1L3 in Ca^{2+}- and Mg^{2+}-dependent cleavage of DNA into oligonucleosomal and high molecular mass fragments. Nucleic Acids Res. 27: 1999–2005
11. Li LY, Luo X and Wang X (2001) Endonuclease G is an apoptotic DNase when released from mitochondria. Nature 412: 95–99
12. Peitsch MC, Polzar B, Stephan H, Crompton T, MacDonald HR, Mannherz HG and Tschopp J (1993) Characterization of the endogenous deoxyribonuclease involved in nuclear DNA degradation during apoptosis (programmed cell death). EMBO J. 12: 371–377
13. Torriglia A, Perani P, Brossas JY, Chaudun E, Treton J, Courtois Y and Counis MF (1998) L-DNase II, a molecule that links proteases and endonucleases in apoptosis, derives from the ubiquitous serpin leukocyte elastase inhibitor. Mol. Cell. Biol. 18: 3612–3619
14. Kovacsovics M, Martinon F, Micheau O, Bodmer J, Hofmann K and Tschopp J (2002) Overexpression of helicard, a CARD-containing helicase cleaved during apoptosis, accelerates DNA degradation. Curr. Biol. 12: 1633
15. Chen J, Jin K, Chen M, Pei W, Kawaguchi K, Greenberg DA and Simon RP (1997) Early detection of DNA strand breaks in the brain after transient focal ischemia: implications for the role of DNA damage in apoptosis and neuronal cell death. J. Neurochem. 69: 232–245
16. Walker PR, LeBlanc J and Sikorska M (1997) Evidence that DNA fragmentation in apoptosis is initiated and propagated by single-strand breaks. Cell Death Differ. 4: 506–515
17. Liu QY, Ribecco-Lutkiewicz M, Carson C, Testolin L, Bergeron D, Kohwi-Shigematsu T, Walker PR and Sikorska M (2003) Mapping the initial DNA breaks in apoptotic Jurkat cells using ligation-mediated PCR. Cell Death Differ. 10: 278–289
18. Yakovlev AG, Wang G, Stoica BA, Boulares HA, Spoonde AY, Yoshihara K and Smulson ME (2000) A role of the Ca^{2+}/Mg^{2+}-dependent endonuclease in apoptosis and its inhibition by Poly(ADP-ribose) polymerase. J. Biol. Chem. 275: 21302–21308
19. Boulares AH, Zoltoski AJ, Contreras FJ, Yakovlev AG, Yoshihara K and Smulson ME (2002) Regulation of DNAS1L3 endonuclease activity by poly(ADP-ribosyl)ation during etoposide-induced apoptosis. Role of poly(ADP-ribose) polymerase-1 cleavage in endonuclease activation. J. Biol. Chem. 277: 372–378
20. de Murcia G and Menissier dM (1994) Poly(ADP-ribose) polymerase: a molecular nick-sensor. Trends Biochem. Sci. 19: 172–176
21. Jeggo PA (1998) DNA repair: PARP–another guardian angel? Curr. Biol. 8: R49–R51
22. Shall S and de Murcia G (2000) Poly(ADP-ribose) polymerase-1: what have we learned from the deficient mouse model? Mutat Res 460: 1–15
23. Masson M, Niedergang C, Schreiber V, Muller S, Menissier-de Murcia J and de Murcia G (1998) XRCC1 is specifically associated with poly(ADP-ribose) polymerase and negatively regulates its activity following DNA damage. Mol. Cell. Biol. 18: 3563–3571
24. Caldecott KW (2001) Mammalian DNA single-strand break repair: an X-ra(y)ted affair. Bioessays 23: 447–455
25. Honda K, Yamada T, Endo R, Ino Y, Gotoh M, Tsuda H, Yamada Y, Chiba H and Hirohashi S (1998) Actinin-4, a novel actin-bundling protein associated with cell motility and cancer invasion. J. Cell Biol. 140: 1383–1393
26. Pandey S, Walker PR and Sikorska M (1997) Identification of a novel 97 kDa endonuclease capable of internucleosomal DNA cleavage. Biochemistry 36: 711–720
27. Walker PR, LeBlanc J, Smith B, Pandey S and Sikorska M (1999) Detection of DNA fragmentation and endonucleases in apoptosis. Methods 17: 329–338
28. Takada F, Vander Woude DL, Tong HQ, Thompson TG, Watkins SC, Kunkel LM and Beggs AH (2001) Myozenin: an alpha-actinin- and gamma-filamin-binding protein of skeletal muscle Z lines. Proc. Natl. Acad. Sci. USA 98: 1595–1600
29. Nikolopoulos SN, Spengler BA, Kisselbach K, Evans AE, Biedler JL and Ross RA (2000) The human non-muscle alpha-actinin protein encoded by the ACTN4 gene suppresses tumorigenicity of human neuroblastoma cells. Oncogene 19: 380–386
30. Suhara T, Mano T, Oliveira BE and Walsh K (2001) Phosphatidylinositol 3-kinase/Akt signaling controls endothelial cell sensitivity to Fas-mediated apoptosis via regulation of FLICE-inhibitory protein (FLIP). Circ. Res. 89: 13–19
31. Bernstein C, Bernstein H, Payne CM and Garewal H (2002) DNA repair/pro-apoptotic dual-role proteins in five major DNA repair pathways: fail-safe protection against carcinogenesis. Mutat. Res. 511: 145–178
32. Trucco C, Oliver FJ, de Murcia G and Menissier-de Murcia J (1998) DNA repair defect in poly(ADP-ribose) polymerase-deficient cell lines. Nucleic Acids Res. 26: 2644–2649
33. Cote J and Ruiz-Carrillo A (1993) Primers for mitochondrial DNA replication generated by endonuclease G. Science 261: 765–769
34. Counis MF and Torriglia A (2000) DNases and apoptosis. Biochem. Cell Biol. 78: 405–414
35. Gavrieli Y, Sherman Y and Ben Sasson SA (1992) Identification of programmed cell death in situ via specific labeling of nuclear DNA fragmentation. J. Cell Biol. 119: 493–501